Optimal Shade Distribution Technique to Mitigate Partial Shading Effects in Photovoltaic Systems

by

Mahdieh Aliaslkhiabani

B.Sc., Central Tehran Branch University, 2014

A THESIS SUBMITTED IN PARTIAL FULFILLMENT OF
THE REQUIREMENTS FOR THE DEGREE OF

MASTER OF APPLIED SCIENCE

in

The College of Graduate Studies

(Electrical Engineering)

THE UNIVERSITY OF BRITISH COLUMBIA

(Okanagan)

December 2018

The following individuals certify that they have read, and recommend to the College of Graduate Studies for acceptance, a thesis/dissertation entitled:

Optimal Shade Distribution Technique to Mitigate Partial Shading Effects in Photovoltaic Systems

Submitted by Mahdieh Aliaslkhiabani in partial fulfillment of the requirements of the degree of Master of Applied Science .

Dr. Liwei Wang, Faculty of Applied Science, UBC Okanagan

Supervisor, Professor

Dr. Martin Ordonez, Faculty of Electrical and Computer Engineering, UBC Vancouver

Co-Supervisor, Professor

Dr. Wilson Eberle, Faculty of Applied Science, UBC Okanagan

Supervisory Committee Member, Professor

Dr. Morad Abdelaziz, Faculty of Applied Science, UBC Okanagan

Supervisory Committee Member, Professor

Dr. Jian Liu, Faculty of Applied Science, UBC Okanagan

University Examiner, Professor

Abstract

Partial Shading (PS) critically reduces the maximum power extractable from a photovoltaic (PV) array, decreasing its efficiency, and creating multiple local peaks (LP) in the characteristic P-V curve of the array. Currently, the electrical connection that minimizes the power loss is the Total Cross Tied (TCT) connection, where each panel in a string is connected in parallel to the all the other panels in the same row, creating an electrical matrix connection. Although the TCT connection reduces part of the problem, it is still sensitive to several shaded panels in the same row constraining the current. In this thesis, a new technique to reduce the consequences of mismatch conditions by optimally distributing the shade over the entire array while maintaining the TCT connection is presented. The proposed method is dubbed "Shade Dispenser" (SD), as it takes a physical shade covering adjacent cells and electrically dispenses it minimizing the occurrence of same-row shades. The physical separation of electrically connected PV panels comes at a cost: it increases the wiring cost and power losses of the array. This trade-off is explored in the proposed paper, outlining the solution for each array size. As a result, this technique represents a considerable reduction in the effects of PS while minimizing wiring losses and costs. The performance of the system is investigated under different shading patterns and compared with the most efficient existing interconnection schemes. Simulation results confirm that not only is the efficiency of the proposed strategy higher, but the payback time for overhead wiring cost is lower. Moreover, this method diminishes the number of Local Peaks (LP) in the P-V curve of the array.

Lay Summary

In PV systems, PS is a common phenomenon which reduces the efficiency of the system to a great extent. PV panels in an array need to be interconnected in series and/or parallel to gain a higher power. The efficiency reduction due to PS is considerably high if the shaded panels are connected in parallel which means that the shade is on some panels which are sharing the same row. This thesis introduces an optimal technique called "SD" to reduce the consequences of PS by distributing the shade over the entire array. Thus, it is guaranteed that those panels which are electrically sharing a row are physically kept far from each other. Another innovation of the proposed method is keeping the series connected PV panels close together to reduce the wiring consumption. Simulation results confirm the effectiveness of the proposed strategy which requires a low payback time for overhead wiring costs.

Preface

This work is based on research performed at the Electrical and Computer Engineering de-partment of the University of British Columbia by Mahdieh Aliaslkhiabni, under the supervision of Dr. Liwei Wang and co-supervision of Dr. Martin Ordonez.

Table of Contents

List of Figures

List of Tables

List of Abbreviations

AC	Alternating Current
AWG	American Wire Gauge
BL	Bridge Linked
DC	Direct Current
FF	Fill Factor
HC	Honeycomb
IESO	Independent Electricity System Operator
I-V	Current-Voltage
KW	Kilo Watt
KWh	Kilo Watt Hour
LH	Long-Horizontal
LP	Local Peak
LV	Long-Vertical
m	Meter
MPP	Maximum Power Point
MPPT	Maximum Power Point Tracker
MS	Magic Square
NP	Number Place
P	Power

PD	Payback Duration
PE%	Power Enhancement
PS	Partial Shading
PV	Photovoltaic
R_s	Series Resistance
R_{Sh}	Shunt Resistance
SD	Shade Dispenser
SH	Short-Horizontal
SP	Series Parallel
SV	Short-Vertical
TCT	Total Cross Tied
W	Watt

List of Symbols

a	Node number
b	String Number
C	Column Number
C_a	Ambient Temperature
C_c	Correction Factor for Semi-enclosed Fuses
C_g	Grouping Correction Factor
C_i	Factor for Conductors Totally Surrounded by Thermal Insulation
i, j, x, y, z	Positive Integer Number
I_L	Line Current
I_c	Cable's Current
I_D	Diode's Reverse Saturation Current
I_G	Photocurrent
$I_{M,N}$	Current of panel M,N
I_{MPP}	Current at the MPP
I_{out}	Output Current
I_{sc}	Short-circuit Current
I_{sM}	String Current
k	Boltzmann Constant
M	Number of Strings in Parallel in an Array
MPP_{Act}	Actual Extracted Power

MPP_{Ext}	Maximum Extractable Power
N	Number of series Connected Panels in a String
n_i	Diode's Ideality Factor
N_{array}	Number of PV Modules Forming the PV Array
n_c	Number of Cable Cores
N_p	Number of Parallel Cells
N_s	Number of Series Cells
pf	Power Factor
$P_{Mismatch\ Loss}$	Power Loss under Mismatch Condition
P-V	Power-Voltage
q	Electron Charge
R_T	Total Number of Rows in an Array
R_θ	Ohmic Resistance of the Conductor at Temperature of θ° C
T	P-N Junction Temperature
V_L	Line Voltage
$V_{m,n}$	Voltage Differences across Panel *m,n*
V_{MPP}	Voltage at the MPP
V_{oc}	Open-circuit Voltage
V_{opt}	Optimal Value
V_{out}	Output Voltage

Acknowledgements

I would like to sincerely acknowledge my supervisor, Dr. Liwei Wang, for his endless supports, encouragement and patient guidance throughout my time as his student. He provided this opportunity for me to work closely with the industry during my degree while was supporting and guiding me from day one.

I must express my gratitude to my co-supervisor, Dr. Martin Ordonez, not only for his excellent technical supervision, but also for his generous supports. It was a precious experience to work in his lab with state-of-the-art equipment.

I would also like to send my special thanks to my parents Behrouz and Safie, my siblings Mahya and Mohamad and all of my family members for their moral and financial supports throughout my life and particularly during my sickness.

I am grateful to Dr. Zahra Arbabian for her time management advices and encouragements throughout this research.

I would also like to thank all the members of Dr. Ordonez's lab for their advices, particularly Ignacio Galiano Zurbriggen and Francisco Paz for their suggestions.

I would like to acknowledge Confirmed Automation Systems for their supports.

Finally, thank you for taking the time to read my thesis.

To my family.

Chapter 1

Introduction

1.1 Motivation

Average electricity consumption has been consistently increasing over the past decade around the world, and Canada is not an exception in this trend. Canadian electricity demand increased by an average of 1.0% per year from 1990 to 2015 [1], and currently, this country is the 9th largest energy consumer in the world [2]. Thus, exploring renewable electricity generation resources is critical to prevent the depletion of fossil fuel reserves, and reduce the environmental concerns. As mentioned in [1], by 2040, 82% of electricity generation in Canada will be from non-emitting sources.

Currently, there are several electricity production methods from renewable sources, but the most significant ones are solar or photovoltaic (PV), wind, geothermal, bioenergy, and hydropower. As reported in [3], renewable energy capacity expansion was significantly higher for the installations of PV energy in comparison with the other resources in the world. Therefore, it is worth spending efforts on efficiency improvements of PV power generation systems especially considering the fact that Canada is planning to rise the PV capacity from 2GW in 2015 to 8-25GW in 2040 [1]. Hence, the major aim of this research is to explore and analyze an approach to improve the efficiency of PV systems under Partial Shading (PS).

Ideally, all PV panels in an array represent the same electrical characteristics; however, practically due to the differences in the irradiance levels caused by snow covering, moving clouds, tree/building shadows, and installing the panels with

different orientations and positions, it is common that in an array some panels receive a different amount of illustrations compared to other ones [16]. Consequently, different output power levels are generated by them. As the shaded panels are electrically connected to another unshaded ones and the same amount of power is not generated by all of them, the panels which generate lower power absorb the power of those which are generating higher energy. Thus, this absorption of the power causes energy loss and hot spot problems. The amount of power loss nonlinearly depends on the shade pattern, array interconnection scheme and the location of shaded modules in the array. It should be noted that the mismatch conditions critically reduces the performance of a PV array if the shaded modules are located in a row [29]-[31].

Researchers have found that the interconnection schemes have a substantial effect on the performance of the PV arrays under PS [5]. The work presented in this thesis introduces a new shade distribution method, called Shade Dispenser (SD), which reduces the effects of PS by distributing the shade over the entire array instead of a single row. Moreover, this new technique reduces the wiring losses and costs compared to other shade distributing methods. Additionally, SD is compatible with all array sizes which is a substantial advantage over the other shade distribution methods. Based on the various case studies performed in this research, SD method enhances the efficiency of the PV array up to 63.7% compared with other conventional methods under PS. Also, in comparison with the recently emerged shade distributing techniques, SD requires up to 87% less wiring requirement.

1.2 Literature Review

The focus of this section is to provide an insight into the recently accomplished researches on enhancing the generated power when PV panels are partially shaded.

Many methods have been proposed to mitigate mismatch losses, and briefly compared in Figure 1.1. In [49], each PV panel is connected to an individual DC-DC converter with a Maximum Power Point Tracker (MPPT) to reduce the effects of PS; however, this method increases the costs of the system to a great extent. Another approach [16], [28], [50]-[53] links the panels through a controllable matrix of switches. Then, by sensing the current and voltage of each panel and based on a controlling strategy interconnects the desired panels. Though this method is able to extract the maximum power out of the array, a large number of sensors and switches are required leading to higher costs and complexity. An alternative method [34] is to utilize a current compensation source to inject current to the shaded panels with lower amount of current. Thus, this technique mitigates the PS losses; however, the required compensation current source, intelligent controller, multiple current sensors and switches make the system costly and complex. Among the existing techniques, shade distribution methods are cheap, maintenance free, and effective to reduce mismatch effects [18], [19]. The logic behind them is to keep the panels electrically connected in the form of total cross tied (TCT) but physically rearrange them to improve the efficiency under PS.

In this section, different commonly used types of interconnection methods and shade distribution techniques to extract the maximum power out of the PV arrays under PS are discussed along with their strengths and weaknesses.

PV array schemes are divided into conventional and shade distributing methods. The most common conventional PV connection topologies are described in details in the following. In addition, some other recently proposed shade distribution techniques

which optimize the operation of the PV system are explained along with their advantages and drawbacks.

Table 1.1: Comparison between PS mitigation methods

	Shade Distribution	Controllable Matrix of Switches	Individual MPPT for each Panel	Current Compensation Source
Extra Circuitry	Not Required	Required	Required	Required
Aging Affect	No	Yes	Yes	Yes
Tuning	Not Required	Required	Required	Required
Maintenance	Not Required	Required	Required	Required
Number of LPs	Medium	Low	Low	Low
Controlling Complexity	Medium	Low	Low	Low
Cost	Low	High	High	High

1.2.1 Common Conventional Interconnection Schemes

Interconnection scheme refers to the configuration of interconnecting PV panels in an array to generate higher output power. Researchers have found multiple configuration techniques for connecting the PV panels together. Among them, Series Parallel (SP), Bridge Linked (BL), Total Cross Tied (TCT), Honeycomb (HC), SP-TCT, and TCT-BL are the most common conventional methods.

In general, these topologies require lower wiring length compare to shade distributing techniques, therefore, their wiring losses and costs are lower. Also, these schemes can be implemented on any array sizes. However, they are unable to distribute the shade over the array; thus, PS can considerably reduce their efficiency.

Moreover, they have a higher number of Maximum Power Points (MPPs) which makes the process of tracking the MPP (MPPT) a complicated tasks resulting in the performance reduction.

- **Series Parallel (SP)**

In SP interconnection configuration, in order to generate higher voltages, PV panels are connected in series and forming strings. Then, strings are connected in parallel to generate higher currents [22], [29]. Generally, it is desired to keep the maximum output current minimum, and maximum output voltage as high as possible. This way, it is not required to use bulky high gauge wires. Therefore, the cost of the system is lower, the power losses of the wirings are minimized, and the system is safer due to less heating.

If an SP connected array has m strings in parallel and each string contains n panels connected in series, it forms an $m \times n$ array [16]. Figure 1.2 represents an array containing 5 panels in series and 4 strings in parallel.

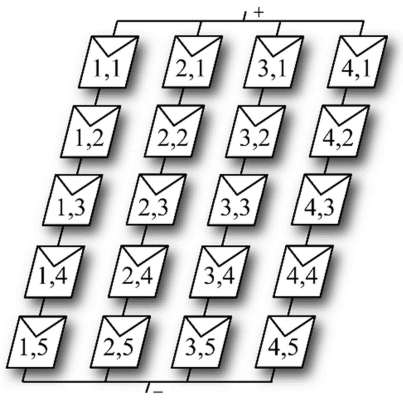

Figure 1.1: SP connection scheme of a 4×5 PV array

The voltage and current relations of this scheme are summarized in (1.1) to (1.3) [7], [18], [25].

$$V_{out} = \sum_{1}^{n} V_{1,n} \tag{1.1}$$

$$I_{sM} = min(I_{m,1}, I_{m,2}, \dots, I_{m,n}) \tag{1.2}$$

$$I_{out} = \sum_{1}^{m} I_{sm} \tag{1.3}$$

Where $V_{m,n}$ and $I_{m,n}$ are voltage differences across panel *m,n* and current generated by the panel, respectively. I_{sm} is the current of each string, and I_{out} is the output current.

In [9], the author evaluates the operation of the SP interconnection method under PS for 3×4 and 6×2 PV arrays under four different shading patterns. This paper firstly explains the reasons of low utilization factor of series connection method mainly in residential areas where many factors may cause partial shading effects, and then suggests connecting the panels in SP scheme instead. The author represents this fact by showing simulation and experimental results of the output power and fill factor of series and SP methods under PS.

Although SP requires low amount of wiring, its performance under PS is very low due to the fact that if one or more panels are shaded they generate lower power and absorb the power of the unshaded panels as there are not enough current paths in this scheme [17].

- Bridge Linked (BL)

The BL scheme, shown in Figure 1.3, is inspired by the wheat-stone bridge connection, and it can be formed by connecting the PV panel in a bridge rectifier

form where two panels are connected in series and then parallel to two strings with a tie between the bridges [4], [30].

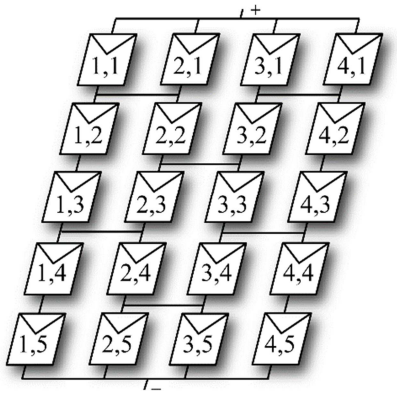

Figure 1.2: BL connection scheme of a 4×5 PV array

By applying Krichoff voltage and current analysis to each four panels of a loop, the voltage and current relations provided in (1.4) and (1.5) can be reached, respectively. It should be mentioned that the output voltage and current relations of BL configuration is the same as SP scheme. In the following expressions, a (where $a = 1, \ldots, m$) is the node number and b (where $b = 1, \ldots, n$) is the string number at the left of the node [11], [21].

$$V_{a,b} + V_{a,b+1} = V_{a+1,b} + V_{a+1,b+1} \tag{1.4}$$

$$I_{a,b}(V_{a,b}) + I_{a,b+1}(V_{a,b+1}) = I_{a+1,b}(V_{a+1,b}) + I_{a+1,b+1}(V_{a+1,b+1}) \tag{1.5}$$

- **Honey Comb (HC)**

HC configuration can be generated by connecting ties across junctions in a honey comb form so that two parallel strings have three series connected modules, shown in Figure 1.4. This interconnection scheme has more internal connections than SP which provides more current paths and further prevents reduction of current in the string. Although the performance of HC configuration is considerably well, there are very

limited numbers of researches carried out on this area [12]. Therefore, to address this limitation, further investigations on this interconnection scheme are done as a part of this thesis.

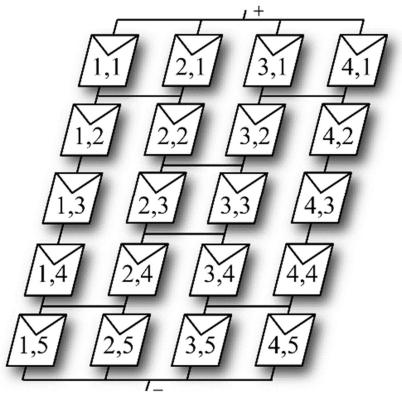

Figure 1.3: HC connection scheme of a 4×5 PV array

Output voltage and output current relations can be found from (1.6) and (1.7), respectively. As can be seen from the equations, the output voltage is equal to the sum of the voltages of the panels in a column, whereas the output current can be calculated by the sum of the currents of the panels in a row.

$$V_{out} = \sum_{1}^{n} V_{m,n} \tag{1.6}$$

$$I_{out} = \sum_{1}^{m} I_{m,n} \tag{1.7}$$

- Total Cross Tied (TCT)

Figure 1.5 shows a TCT configuration which connects all columns of a PV array in series and rows in parallel, and forms a matrix-like connection. As a result, it is characterized as the scheme that requires the highest amount of wiring. The effects of PS on this scheme is low [17] because the interconnection between the PV strings balances the effects of non-uniform illustration level across each ties in TCT [10].

Also, in general, topologies with higher interconnections take advantage of less possibility of turning on the bypass diode, thus reducing mismatch losses, hot spots, and the multi-peak effects.

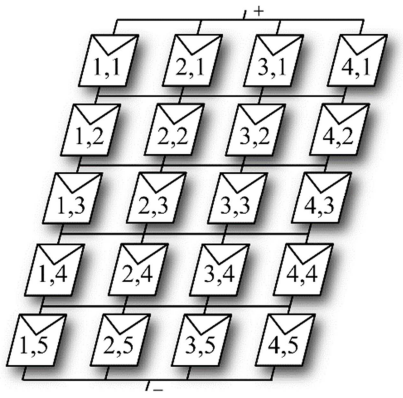

Figure 1.4: TCT connection scheme of a 4×5 PV array

The voltage and current relations of a TCT configuration are similar to SP interconnection scheme, calculated in (1.1) to (1.3), which the sum of cell currents along any row is the array current, and the sum of cell voltages along any column is equal to the array terminal voltage [4], [7], [8].

- **SP-TCT**

In [27] a topology called SP-TCT is proposed. This scheme is a combination of SP and TCT schemes. The internal connections of this topology are lower than TCT, and higher than SP. Therefore, the current path and wiring cost of this topology is higher than SP, and under PS, it is expected to have a better efficiency than SP; however, the wiring cost and the under PS efficiency of this method is lower than TCT due to lower number of current paths. Figure 1.6 shows a SP-TCT configuration for a 4×5 PV array. The voltage and current relations of a SP-TCT configuration are similar to SP scheme.

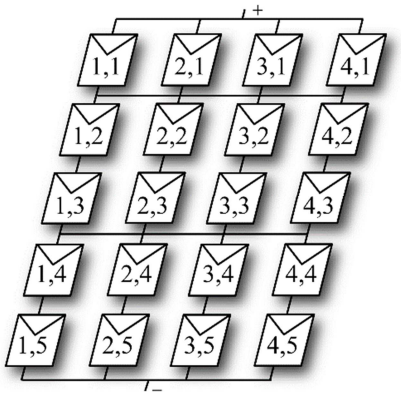

Figure 1.5: SP-TCT connection scheme of a 4×5 PV array

- TCT-BL

Figure 1.7 presents a recently emerged scheme called TCT-BL which is reported in [27]. Similar to the previous topology, this interconnection configuration also tries to improve the efficiency of the panels under PS by providing more current paths than BL topology and lower wiring connections than TCT scheme. Therefore, it is expected that TCT-BL has a higher efficiency and cost compared with BL pattern, and lower wiring cost and performance than TCT method when partially shaded. In TCT-BL topology, the voltage and current relations are similar to SP scheme.

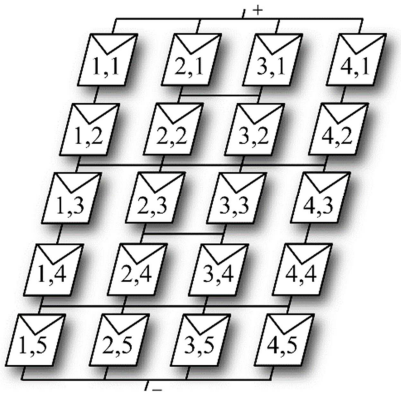

Figure 1.6: TCT-BL connection scheme of a 4×5 PV array

1.2.2 Shade Distributing Techniques

Shade distributing schemes are reported to have a higher efficiency compared to conventional methods under PS [18]-[20]. Additionally, due to their capability in distributing the shade over the entire array, the possibility of turning on the bypass diode is lower resulting in a reduction in the number of Local Peaks (LP) in the P-V curve of the system which makes MPPT a simpler task resulting in a more efficient and less complex system. Figure 1.8 represents the concept behind shade distribution techniques and the advantages of implementing them.

The existing techniques are called Number Place (NP), Magic Square (MS) and Su Do Ku which are discussed in the following.

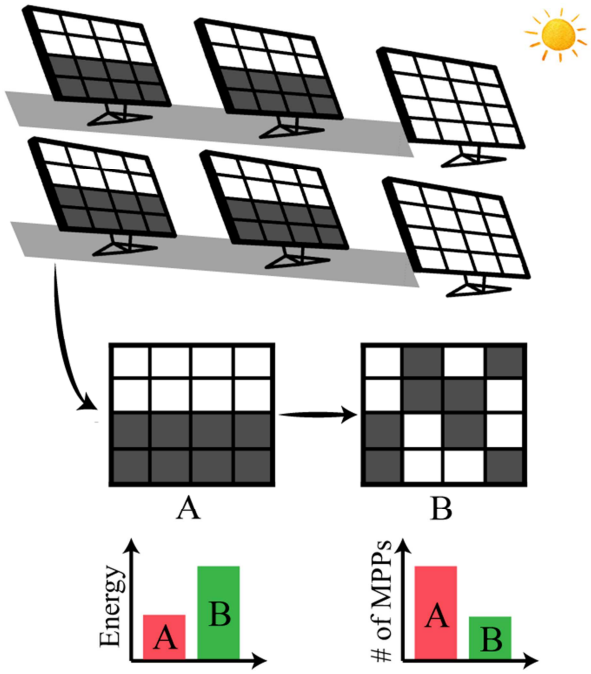

Figure 1.7: PS effect on several panels in an array resulting in a lower power generation. Energy can be enhanced by utilizing a shade distribution technique while reducing the number of LPs.

- **Number Place (NP)**

This method which is reported in [29] gives a digit from 1 to 6 to each row and column of a 6×6 TCT array, and rearranges the panels so that no digit repeats in any row or column. Therefore, the locations of the panels are changed but the electrical connections remain the same as TCT pattern. Simulation results in [29] show up to 6.7% improvement in the output power of a 6×6 PV array shown in Figure 1.9. As can be seen, each row and column of a branch consists of all the digits from 1 to 6 [29]. The voltage and current relations of this method are the same as TCT configuration as the electrical connections are the same a TCT.

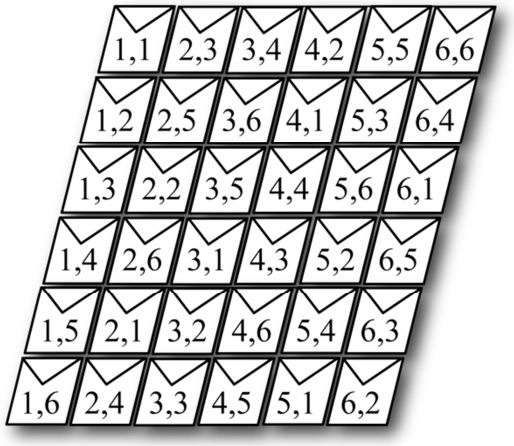

Figure 1.8: Number Place shade distribution method for a 6×6 PV array

One of the weaknesses of this algorithm is the requirement of a large amount of wiring which causes wiring losses in the system, and increases the cost. Another disadvantage of this method is that it only works for a 6×6 PV array. In fact, the author has provided no method which is compatible with other array dimensions.

- **Magic Square (MS)**

In [30], another shade distribution technique called Magic square is proposed. This method is suitable for any $j=(2i+1)$ with i being a number from 1 to i^2 in an $j\times j$ TCT connected array which reconfigures the panels in the array in a way that the sum of the entries of any row, any column, or any main diagonal stay equal. The arrangement of the panels in MS technique for a 5×5 array is shown in Figure 1.10. As can be seen in the figure, this method puts the array number 1 in the middle of the first column, then, places the next panel number on the down left side of the current panel. If that place is already filled by another panel, the next panel should be placed on the immediate right side of the current panel. It should be noted that this method considers a "wrap-around" the array, so if any panel is moved off one side of the array, it re-enters from the opposite side [30].

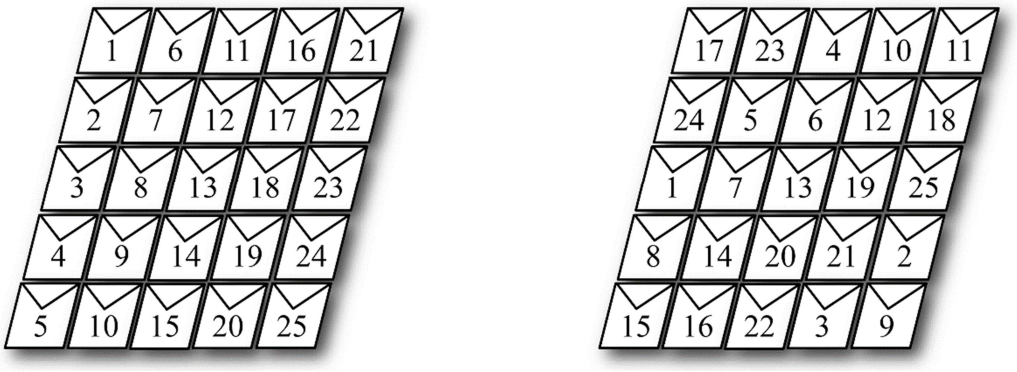

(a) (b)

Figure 1.9: Magic Square shade distribution method for a 5×5 PV array, (a) TCT non-reconfigured array, and (b) reconfigured array

Similar to previous shade distribution techniques, this method also keeps the electrical connections the same as TCT scheme, and physically relocates the panels to reduce the PS effects on a single row. Thus, the effects of PS are reduced by

increasing the incoming current at a particular node which lessens the bypassing of the panels. Based on the report in [30], this shade distribution method show at least 5.88% efficiency improvement compared to TCT scheme. It should be mentioned that voltage and current relations of MS are also the same as TCT scheme. The main drawbacks of this technique are similar to that of the NP method which was described in the previous section.

- **Su Do Ku**

Another shade distribution method, proposed in [31], is called Su Do Ku. In this technique, the PV arrays are rearranged based on the Su Do Ku puzzle pattern which consists of nine 3×3 matrices. In this puzzle, each row, column, and 3×3 matrix contains all of the digits from 1 to 9 with no repeated digit. This pattern is shown in Figure 1.11 for a 9×9 PV array. Similar to the two previously mentioned shade distribution methods, the electrical connections of this technique remains the same as TCT scheme, and only the physical placements of the PV panels are reconfigured. Therefore, voltage and current relations of this technique are also the same as TCT configuration. This method distributes the shade over the entire array by ensuring that the panels in a row are kept apart which improves the power generated by the array for the same shading pattern. Based on the results shown in this study, Su Do Ku pattern can enhance the efficiency by 3.6% and higher.

One of the main downsides of this method is the huge selected PV array size which may not be suitable for small residential PV plants. Also, this method only considers a specific PV array size which limits the designers. Additionally, the panels in Su Do

Ku technique are kept very far from each other and have a high wiring length; however, the wiring losses are not considered in [31].

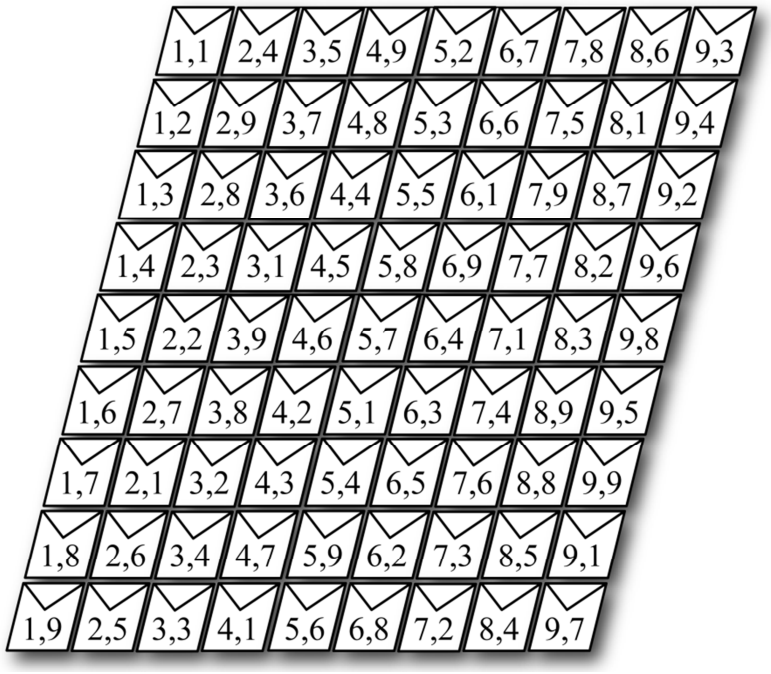

Figure 1.10: Su Do Ku shade distribution method for a 9×9 PV array

One of the main downsides of this method is the huge selected PV array size which may not be suitable for small residential PV plants. Also, this method only considers a specific PV array size which limits the designers. Additionally, the panels in Su Do Ku technique are kept very far from each other and have a high wiring length; however, the wiring losses are not considered in [31].

1.2.3 Summary

As PS substantially affects the efficiency of the PV systems, in this this literature review the existing methods to enhance the output power were discussed along with their strength and weaknesses. Among them, shade distribution methods were better

candidates to mitigate shading effects due to less complexity and cost. However, the existing shade distributing techniques require a large amount of wiring length and are incompatible with all array sizes which remain many challenges open. Therefore, a high efficiency reconfiguration method with minimal wiring length compatible with all array dimensions is lacking in the literature. Consequently, these challenges are addressed in this research.

1.3 Thesis Outline

This thesis is organized into five chapters as follow:

- Chapter 1 explains about the motivation of this research. Afterwards, a literature review is discussed containing an explanation about the existing methods to mitigate PS effects. In addition, the common conventional topologies to interconnect the PV panels and recently emerged methods to distribute the shade are discussed in details.
- In chapter 2, a brief background of PV systems, and an insight into the electrical characteristics and modelling of a PV array under different environmental conditions are mentioned. Then, the effects of wiring losses and irradiance transient losses due to mis-selection of MPPT under PS are introduced.
- Chapter 3 describes a proposed interconnection method which improves the efficiency of the PV arrays under PS, and reduces the wiring requirements and costs.
- In chapter 4, the interconnection schemes are simulated in MATLAB/Simulink, and multiple comparisons of the efficiency of the topologies are done. To provide more accurate results, different PV array sizes under various shading patterns are studied.

- Chapter 5 makes comparison of the payback duration for the increased wiring cost of different interconnection schemes including the presented method.
- In chapter 6, this thesis work is summarized and concluded and some of the possible future directions of the work for further efficiency enhancement are outlined.

Chapter 2

PV Systems Background and Energy Harvesting Losses

In PV power generation systems, PV arrays, connected to DC-DC converter with a smart controlling system for extracting the maximum power from the panels, convert the solar irradiance into electricity [36]. Afterwards, based on the configuration of the PV system, the generated electricity which is a Direct Current (DC) type should be stored in batteries or converted to Alternating Current (AC) and fed into the local loads and/or the gird. Figure 2.1 shows the basic structure of a grid-connected PV plant with energy storage system.

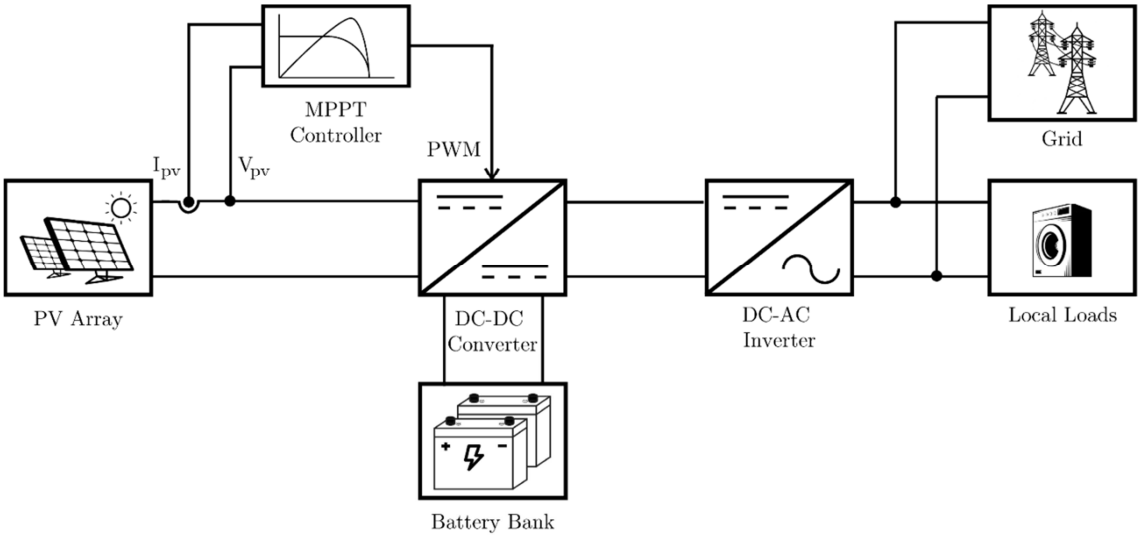

Figure 2.1: Basic configuration of a grid-connected PV system with energy storage

This chapter provides an insight into the electrical characteristics and modeling of PV arrays under different environmental conditions. Also, the effects of wiring losses and PS phenomenon on the performance of the PV systems are discussed.

2.1 PV Array Electrical Characteristics and Modeling

PV cells are connected in series and parallel for higher output voltage and current, respectively, and form a PV module. To achieve higher power, several modules may be grouped in series or parallel which forms PV panels and arrays [32].

Due to the nonlinear characteristics of PV cells, it is necessary to model them for simulating a PV system [6]. This can be done by considering its equivalent circuit, shown in Figure 2.2. At constant temperature, when the irradiation level increases, PV cell produces a current corresponding to that irradiation. Hence, the ideal PV cell can be modeled as a current source anti-parallel with a diode. However, in practice no solar cell is ideal. Thus, a shunt resistance (R_{Sh}), and a series resistance (R_s) are required to be added to the model. R_{Sh} creates a path around the PV cell junction without producing power which leads to short circuiting the current within the cell, and reducing the performance [35]. In ideal conditions, the value of the R_{Sh} and R_S should be infinite and zero, respectively so that the chance of current flow through the R_{Sh} is nearly zero, and the power loss around R_S is minimized [37].

The most common electrical models for PV cells are single-diode and two-diode [38]. Two-diode model has an additional diode compared with a single-diode which further refines the operation of the PV cells by providing a more accurate I-V curve. However, under Standard Test Conditions (irradiance = 1000W/m^2, temperature = 25°C, and solar spectrum=1.5) the simulation results of the two

models are almost similar [32]. Thus, for most studies a PV model with a single diode is sufficient [39], [46], and this thesis is not an exception. The output current of the single diode model is formulated in (2.1) [8], [16], [40].

$$I_{out} = I_L - I_D\left(e^{\frac{q(V_{out}+IR_s)}{nkT}} - 1\right) - \frac{V_{out} + IR_s}{R_{sh}} \tag{2.1}$$

Where I_L is the photocurrent, I_D is the reverse saturation current of diode, q is the electron charge, k is the Boltzmann constant, T is the p-n junction temperature, and n is the ideality factor of the diode which is 1 if the transport process is purely diffusion, and 2 if it is primarily recombination in the depletion region. For silicon solar cells ideality factor is 1.3 [39], [40].

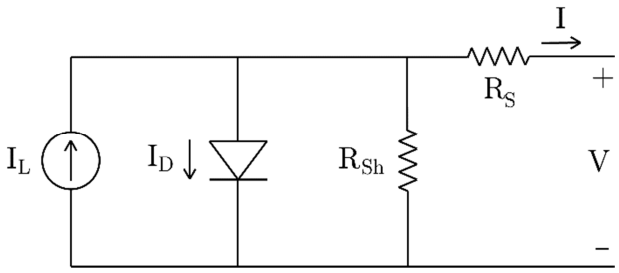

Figure 2.2: Single-diode PV cell equivalent circuit models

For modeling the behaviour of a PV system, a PV array which consists of a number of PV cells connected in series and parallel should be modeled as the power of a PV cell is too low. The output voltage of an array is equal to the voltage of an individual cell by the number of cells connected in series, and its output current is the product of a cell current by the number of cells connected in parallel. For a PV array with N_s number of series cells and N_p number of parallel cells, (2.1) can be rewritten as (2.2) [32], [40], [41].

$$I_{out} = N_p I_L - N_p I_D\left(e^{\frac{q\left(V+IR_sN_s/N_p\right)}{nkT}} - 1\right) - \frac{V + IR_sN_s/N_p}{R_{sh}N_s/N_p} \tag{2.2}$$

Figure 2.3 shows the I-V operating characteristics of a PV array consists of two 335 W panels, with R_s and R_{sh} equal to 0.1 Ω and 1 KΩ, respectively. In part (a), the PV characteristic is plotted under different irradiance levels, and in part (b), under different temperature values. As can be seen, variations in the irradiance level influence the output current. Contrarily, the effect of the changes in temperature is on the output voltage [23].

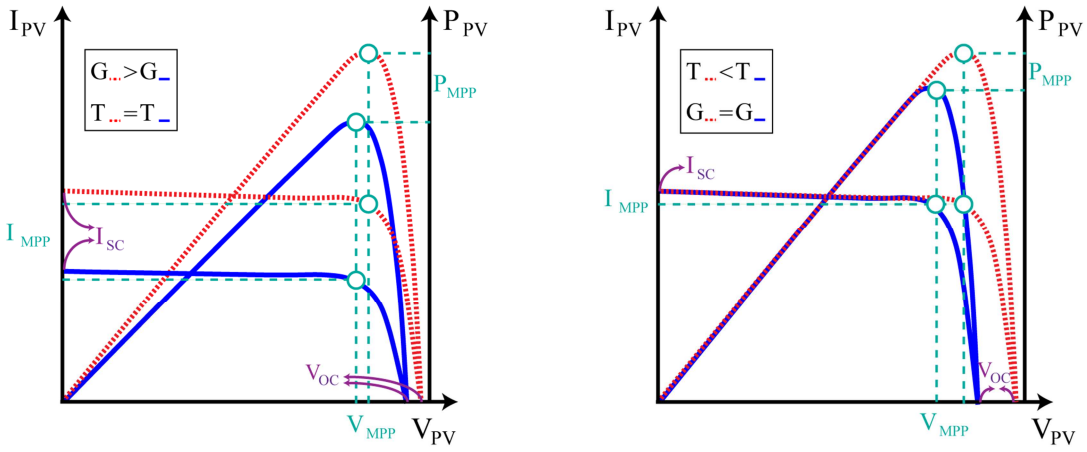

(a) (b)

Figure 2.3: The I-V curve of two 335 W PV panels under different: (a) irradiation levels with constant temperature (25°C), and (b) temperature values with constant irradiance (1000 W/m^2)

I-V and P-V curves provide three key operating points, namely short-circuit current (I_{sc}), open-circuit voltage (V_{oc}), and Maximum Power Point (MPP), which are widely used to design a controller to extract power from the PV panels. These three points are shown in Figure 2.4 [10], [32]. MPP is the area under the I-V curve which is maxima. Also, as can be seen in part (a) of the figure, MPP is the highest possible extractable power from the PV panels. Thus, form the P-V curve of the panel, the voltage at the MPP (V_{MPP}) can be found. Then, by knowing the V_{MPP}, the current at the MPP (I_{MPP}) can be calculated from the I-V curve shown in part (b) [41].

It should be mentioned that due to the components' losses, the amount of V_{MPP} and I_{MPP} are always lower than V_{oc} and I_{sc}, respectively. Therefore, a widely used measure in PVsystem called Fill Factor (FF), is used which shows the ratio of the actual MPP to the theoretical one and is formulated in (2.3) [42].

$$FF = \frac{V_{MPP} \times I_{MPP}}{V_{OC} \times I_{SC}} \tag{2.3}$$

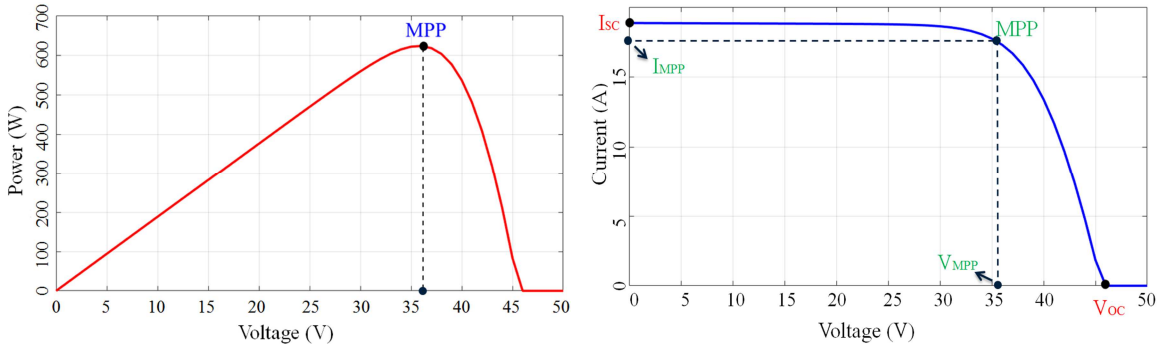

(a) (b)

Figure 2.4: Significant operating points of a PV panel illustrated in: (a) P-V curve, and (b) I-V curve

2.2 Cable Selection and Power Losses

Cables provide connection and safe passage of current between the components in a PV system, and must be selected appropriately based on their application and sizing. Undersize or inappropriate wire selection can cause severe damages to the PV system. The size of the wire can be determined by estimating the maximum voltage, current, transmission length, and temperature [44]. (2.4) and (2.5) formulate the current relation based on the power usage of the loads, voltage and different applicable correction factors for thermal insulation and re-wirable fuses for a single-phase and three-phase system, respectively [45].

$$I = \frac{P}{V \times pf \times C_a \times C_g \times C_i \times C_c} \tag{2.4}$$

$$I_L = \frac{P}{\sqrt{3}V_L \times pf \times C_a \times C_g \times C_i \times C_c} \tag{2.5}$$

Where pf is the power factor, V_L and I_L are the line voltage and current, respectively. Also, C_a is ambient temperature, C_g is grouping correction factor, and C_i is the factor for conductors totally surrounded by thermal insulation; the amount of this factor is selected to be 0.5. Finally, C_c is the correction factor for semi-enclosed fuses. The amount of these factors can be found in the appendix parts of [45]. After calculating the current flow in the cables, an 80% margin is usually added to the amperage tolerance of the cable.

Wire Losses are ohmic losses and happen due to raising current which generates heat and resistivity in the cable and can be calculated from (2.6) [47]. It should be mentioned that higher gauge cables have lower power loss; however, as the cable cost increases by gauge size increment, a balance between efficiency and cost should be maintained in PV systems.

$$P_{Cable\ Loss} = n_c {I_c}^2 R_\theta \tag{2.6}$$

Where n_c is the number of cable cores, I_c is the current carried by the cable and R_θ is the ohmic resistance of the conductor at temperature of θ°C.

2.3 Mismatch Power Losses

PS is a common phenomenon that occurs when a portion of PV panels in an array receive a different amount of irradiation [48]. As the current generated by the PV panels is proportional to the solar insolation level, PS reduces the photocurrent generated by the PV cells [26]. Also, the shaded panels become reverse biased, and act as a load to absorb the power, and if they are connected in series, they limit the string current of the array leading to the reduction in the maximum extractable power level [34]. For instance, one fully shaded panel can reduce the output power by 40% to 95% [43]. This fact may substantially affect the performance of the PV system and cause instability, therefore, a proper size and scheme selection for the PV array is critical [6]. The power that is lost in this way is called mismatch loss and is formulated in (2.7) [23], [33], [48] and shown in part (b) of the figure. Additionally, the efficiency improvement or the percentage of the power enhancement (PE%) can be found from (2.8) [55].

$$P_{Mismatch\ Loss} = \sum_{n=1}^{N_{array}} MPP_{Ext} - MPP_{Act} \tag{2.7}$$

$$PE_{\%} = \frac{MPP_1 - MPP_2}{MPP_2} \times 100 \tag{2.8}$$

Where N_{array} is the number of modules forming the PV array, MPP_{Ext} and MPP_{Act} are the maximum extractable power of the PV array and its actual power, respectively. In residential systems, it is common to see a large amount of power loss under PS [23]. Also, it is pointed in [48] that the mismatch losses are zero when all panels in an array are unshaded or fully shaded.

It should be mentioned that if the reverse bias voltage of partially shaded cells is too high, the cell may enter the avalanche breakdown region which may cause irreversible damage to the cell. This so-called hot spot can be avoided by connecting a bypass diode anti-parallel to one panel or a set of series connected panels to limit the reverse voltage [13]. However, the bias voltage of the bypass diode affects the operating voltage of the cell leading to multiple peaks in the panel's P-V curve which makes MPPT a difficult task, consequently, reducing the output power [13], [16], [34], [43]. Generally, in the arrays with higher interconnection numbers, as there are more current flow paths which reduces the power losses [10].

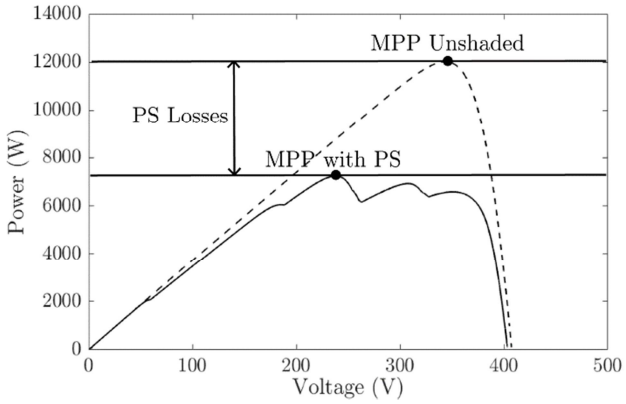

Figure 2.5: Comparison between the P-V curves of unshaded and partially shaded PV array [28]

2.4 Summary

This chapter provided a background about the electrical characteristic of PV cells and their important operating points. Also, two commonly used PV cell equivalent circuit models were explained and among them the single-diode model was selected as the best possible model due to less complexity which reduces the simulation time. Then, the equation to model a PV array was represented followed by a simulation of a 335

W PV panel under different environmental conditions. Based on the investigations in this part, variations in the irradiance level influenced the output current, and the effect of the changes in temperature was on the output voltage. Moreover, a guide to calculate the current tolerance of a conductor is explained followed by an equation to find the cable losses. Finally, this section was concluded by a discussion about the effects of PS on the performance of the PV system.

Chapter 3

Shade Dispenser Technique

As discussed before, the mismatch condition critically reduces the performance of a PV array if the shaded modules are located in a row [30], [39], [46]. Therefore, in this thesis, a new method called SD is presented to reduce the effects of PS. In this technique, the panels are connected in the form of TCT; however, their physical locations are changed, so that the shade is distributed over the entire array instead of one or more rows. Another key feature of SD shade distribution technique is the minimal displacement of the series connected panels in an array which reduces the wiring losses and costs compared to other shade distribution methods. Another unique characteristic of this technique which is a substantial advantage of SD over the other shade distribution methods is its capability to be implemented on any array sizes. Additionally, SD technique reduces the number of LPs in the P-V curve of a PV array due to lower possibility of turning on the bypass diode.

3.1 Shade Distribution Strategy - Flowchart and Patterns

The SD panel displacement technique interconnects the PV panels in the form of TCT and optimally reconfigures their physical locations in an array to distribute the shade. In this method, each panel has a column number (C). As the effect of PS on some panels which are located on a shared column is considerably low, not only does

moving the panels out of their column have no positive effect, but also it adds the costs and losses of the system due to higher wiring length. Therefore, similar to Su Do Ku and NP methods, in SD technique, panel shade distribution happens within each column, and no panel moves out of its column.

The main disadvantage of the other methods in the literature is that the series connected panels are far from each other resulting in higher losses, wiring complexity, and longer payback duration. Therefore, the main innovation of SD method is to keep the series connected panels close together while distributing the panels within their column. Thus, the strategy of this technique is to move up all panels in a column by an optimal value (V_{opt}). To find this amount, an optimization problem needs to be solved which simultaneously takes into account the two following objective functions.

1- Wiring length: It is desired to keep the wiring length minimum as lower wiring length reduces the overhead wiring costs of the system leading to shorter payback duration, and minimizes the wiring losses.

2- Distance between the panels located on a shared row: The main objective of shade distribution techniques is to wire (or rewire) the array in a way that those panels which are electrically sharing a row are physically located as far as possible from each other which mitigates the effects of PS.

To solve this multi-objective optimization problem, Pareto optimization method is selected to find V_{opt} in the presence of a trade-off between a short wiring length and a long distance between the panels. To solve this problem, those two objective functions are calculated for different array sizes. For this experiment, as the column number is not a major factor, it needs to be a constant value to be able to find out the relation between V_{opt} and the total row numbers. Therefore, 11 columns are considered here, and the relation between wire length, distance between the panels

and V_{opt} for all possible total number of rows from 1 to 49 are investigated, and represented in Figure 3.1. As can be seen, there is a boundary, shown with dashed red line, where the distance between the panels are maximum and the wiring length is minimum. This boundary determines the feasible choice to move the panels.

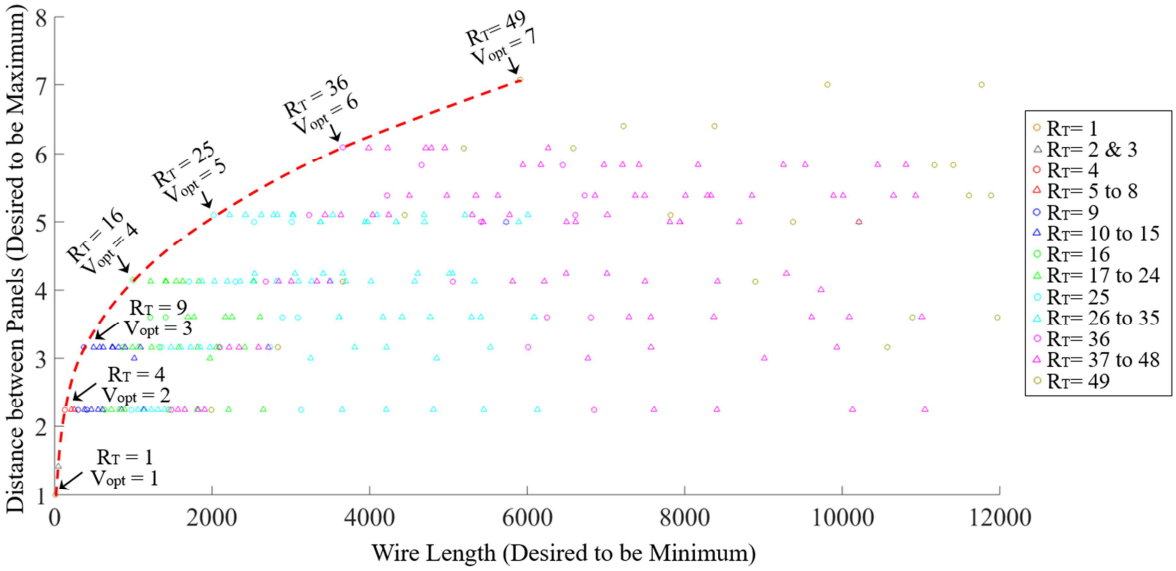

Figure 3.1: Pareto optimization plot considering the wiring length and the distance between the panels as the objective functions to find the optimal value based on the total number of rows in an array to move the panels up within their column

To formulize this feasible choice for V_{opt} based on the above figure, first it should be found out if there is a positive integer (x) so that (3.1) and (3.2) are satisfied.

$$R_T = x \times y \quad x, y \in N \Leftrightarrow R_T | y \tag{3.1}$$

$$\lfloor \sqrt{R_T} \rfloor = x \times z \quad x, z \in N \Leftrightarrow \lfloor \sqrt{R_T} \rfloor | z \tag{3.2}$$

Where R_T is the total number of rows in an array, and y and z are positive integer numbers.

Then, if there is not any x to satisfy the above equations, panels need to move up by V_{opt} which is formulized in (3.3). However, if there exists an x, moving the panels up by (3.3) puts multiple panels with the same row number again on the same shared row which reduces the efficiency. Thus, an extra part is required to be added to the equation for better array distribution. Therefore, moving the panels up by (3.4) shows a better behaviour. It should be noted that the columns in the SD method are considered to wrap around such that if a panel moves out of one side of a column it re-enters from the other side. Figure 3.2 represents the flowchart of this algorithm.

$$V_{opt} = (C-1) \times \lfloor \sqrt{R_T} \rfloor \tag{3.3}$$

$$V_{opt} = (C-1)\lfloor \sqrt{R_T} \rfloor + \left\lfloor \frac{C-1}{\lceil \sqrt{R_T} \rceil} \right\rfloor \tag{3.4}$$

For further clarification, Figure 3.3 shows two examples of the operation of this algorithm for a 3×5 and 4×4 PV array considering the wiring connections. For a 3×5, as there is no x satisfying (3.1) and (3.2), V_{opt} can be found from (3.3). However, for a 4×4 array, x is equal to 2, therefore, (3.4) should be used. It should be noted that for this array size, if (3.3) is used panel 1,1 and panel 3,1 will be on the same shared row which is not desired but using (3.4) guarantees no panels with the same row number on a shared row.

It should also be mentioned that as the electrical connections of this shade distribution method remain the same as TCT scheme, the current and voltage relations remain the same as the TCT configuration which was discussed in chapter 1.

Therefore, SD improves the power generated by the array for the same shading pattern by ensuring that the panels in a row are kept apart from each other which distributes the shade over the entire array.

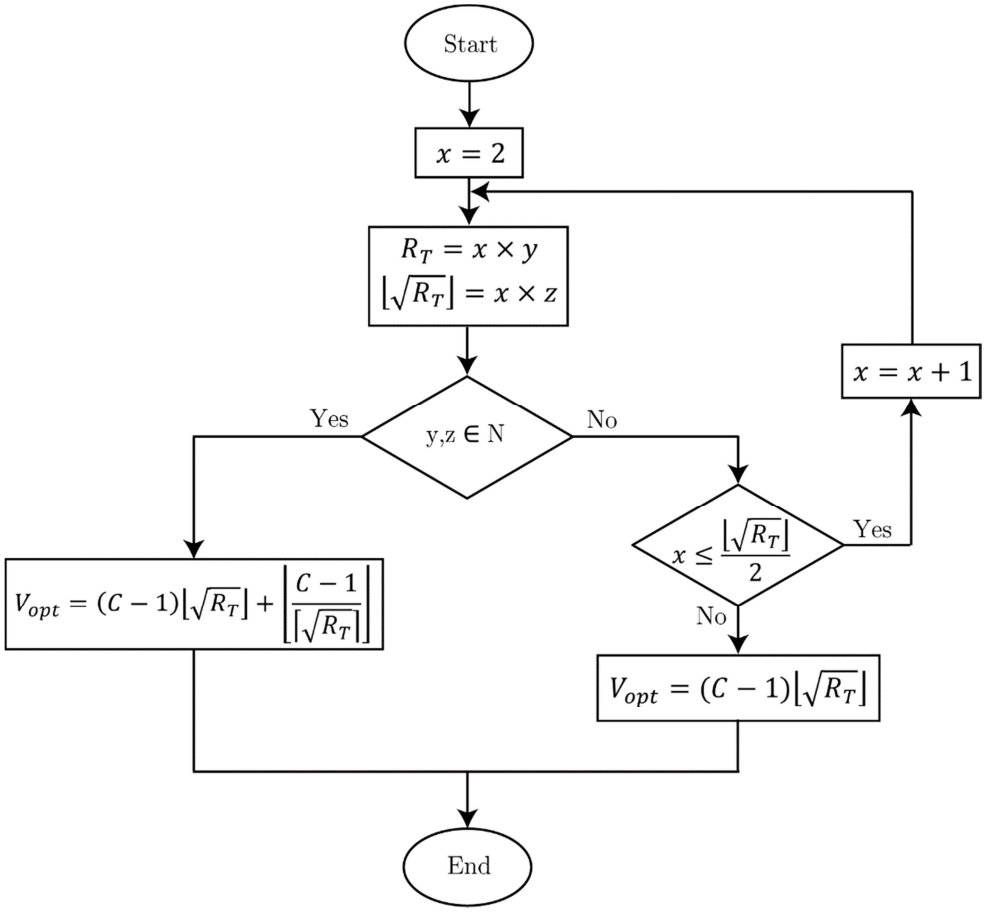

Figure 3.2: Flowchart of SD algorithm of an $m \times n$ PV array

The advantages of SD over the other interconnection schemes which are not capable of distributing the shade over the entire array, is reducing the effects of PS on a row which enhances the efficiency of the PV system by generating more power. Simulation results shown in chapter 4 represent that when wiring losses are considered, SD technique improves the efficiency of the PV array up to 63.7% compared with other the methods under PS. Although the cost of wiring is higher in SD technique, based on the case studies investigated in chapter 5, this overhead cost

can be covered in less than two years by more power generation. Therefore, as the period of the operation of PV panels is nearly 25 years [18], the system pays back for its wiring overhead costs very fast, so the benefits of this technique is considerably higher than the other mentioned interconnection methods.

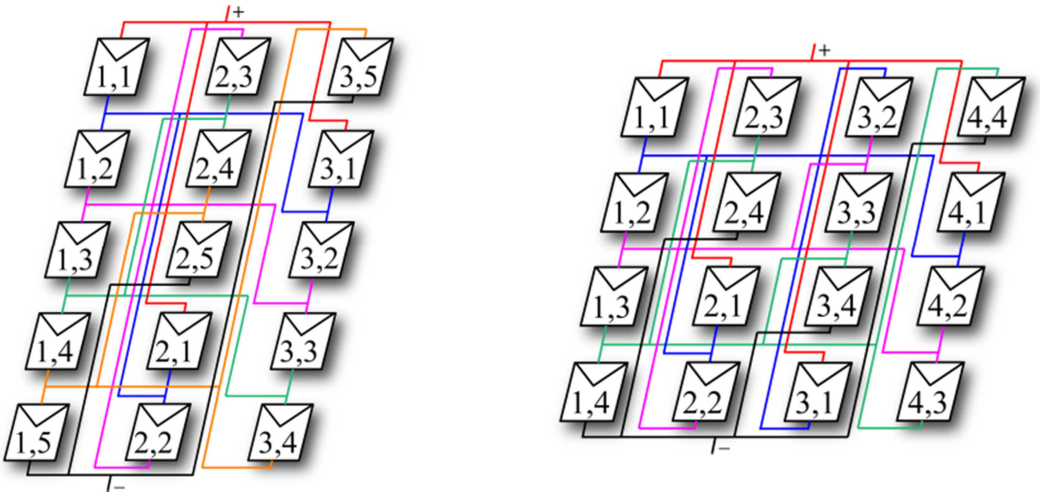

(a) (b)

Figure 3.3: Wiring connections of SD shade distribution technique for a (a) 3×5 PV array, and (b) 4×4 PV array

Comparing SD strategy with other shade distribution techniques indicates that as SD has a lower number of movements, it requires lower wiring. Therefore, it has less wiring losses and costs. Also, due to the reduction in the wiring losses, the simulation results show up to 17.7%, 7.4%, and 8.4% efficiency improvement compared with NP, MS, and Su Do Ku methods under PS, respectively. Additionally, as the wiring complexity of this technique is minimized, the installation costs are also lower.

3.2 Brief Comparison Table

Table 3.1 briefly compares the SD technique with other interconnection methods. It should be mentioned that detailed comparisons are presented in chapter 4 and 5.

Table 3.1: Comparison between different interconnection schemes under PS

Scheme Type	Efficiency Improvement	Wiring Investment Return	Compatible with all Array Sizes	Number of MPPs
SP	Very Low	Fast	Yes	High
BL	Low	Medium	Yes	High
TCT	High	Slow	Yes	High
HC	Low	Medium	Yes	High
SP-TCT	Medium	Slow	Yes	High
TCT-BL	Medium	Slow	Yes	High
NP	Very High	Fast	No	Low
MS	Very High	Very Slow	No	Low
Su Do Ku	Very High	Medium	No	Low
SD	Very High	Very Fast	Yes	Low

As can be seen in the table, the other advantage of SD technique is having a lower number of LPs in the P-V curve of the PV array compared with other conventional schemes. In general, systems with higher capability of distributing the shade show a lower number of LPs. The main advantage of this phenomenon is the requirement of a simpler, faster and more efficient MPPT controller which reduces the costs and complexity of the system while enhancing the output power. Therefore, as SD technique has a better capability in shade dispensing, it has the minimum number of LPs among the other methods.

3.3 Summary

In this chapter, SD shade distribution method is proposed to reduce the power losses of PS by distributing the shade over the entire array by minimally relocating the PV panels inside an array and keeping them electrically connected in the form of TCT interconnection scheme. This technique improves the efficiency of the PV panels up to 63.7% under PS compared with other interconnection schemes which are not capable of distributing the shade. Also, in comparison with the other shade distribution methods, SD requires up to 87% less wiring which reduces the system complexity, wiring losses and cost.

Additionally, different interconnection schemes are compared briefly in Table 3.1. A positive point of the SD method is its low peak numbers which makes the MPPT more efficient due to lower LPs. Although the wiring cost of SD is high, the PV system pays back for this overhead cost in less than two years by generating more power.

Chapter 4

Simulations

Due to the high costs of PV systems, it is significant to analyze and compare the operation of different interconnection schemes of an array under PS to extract the maximum possible power out of the PV panels. As field testing is costly, time-consuming, demanding, and dependent on weather conditions, performing investigation on physical PV module seems impossible, and using simulation tools is a better choice [29], and [46]. Therefore, the main purpose of this chapter is to make comparisons between SD technique, conventional interconnection schemes, and recently emerged shade distribution methods, explained in the previous chapters, under different shading patterns using MATLAB/Simulink.

In this research, to ensure the power increment by the proposed shade distribution strategy, all possible vertical and horizontal shading patterns are considered for two different array dimensions. It should be noted that for the simulation, each selected panel is capable of generating maximum of 335 W. Therefore, the maximum power generation by a 6×6 PV array is 12.06 KW and a 9×9 PV array is capable of producing maximum 27.135 KW.

Additionally, in this section, the efficiency improvement by SD method is evaluated for a case study. In this study, the PV panels installed on the roof of the North Vancouver Library are considered which are shaded by the surrounding buildings, and the efficiency improvement of SD is compared with the most efficient conventional interconnection scheme, TCT, during a summer day. It should be

mentioned that the shade distribution strategies are not considered for this case study due to their incompatibility with the array size of this plant.

4.1 Power Enhancement Evaluation for All Possible Horizontal and Vertical Dimensions of Shadows

In this section, to accurately compare the operation of the SD technique with other interconnection schemes and shade distribution techniques, all possible shading patterns of a 6×6, and 9×9 PV array are evaluated. It should be mentioned that to achieve more accurate results, the wiring losses are included in the simulations. Additionally, 3 dimensional figures are used to present the simulation results in a compact way.

- **6×6 PV Array**

Figure 4.1 represents the PE% of 324 different shading patterns for a 6×6 PV array with different interconnection configurations. Due to the array size limitations, Su Do Ku and MS shade distribution techniques are not considered here and only the performance of conventional schemes and NP are compared with SD method. As can be seen in part (a) of the figure, under PS, SD shade distribution technique is capable of improving the output power by the maximum of 63.7%. Simulation results, shown in part (g), represents up to 17.7% efficiency improvement by SD compared to NP shade distribution method.

To model the wiring losses, the short circuit current of the PV array is measured which is 37 amp for this array size, thus, an 8 AWG wire which is capable

of handling 40 amp current should be selected. The material of the wire is chosen to be cooper, therefore, the wire resistance is 2.061 ohm per 1000 m.

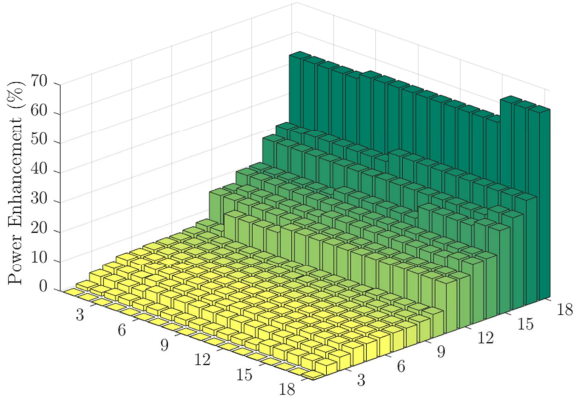

(a)

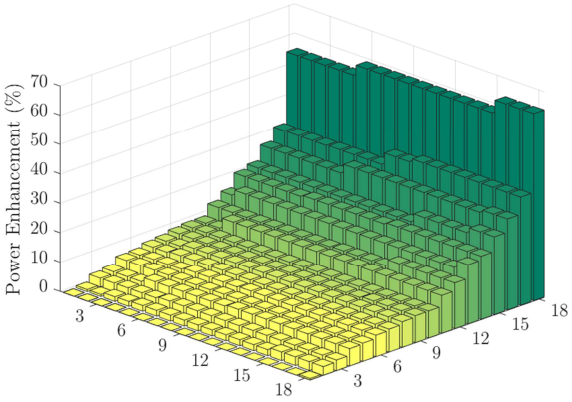

(b)

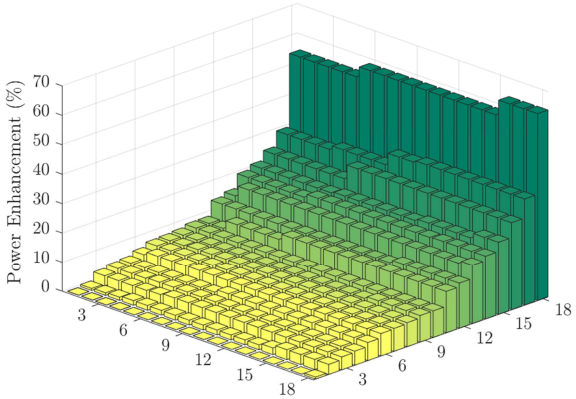

(c)

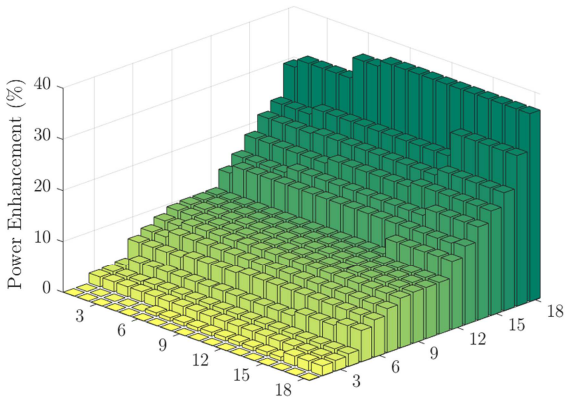

(d)

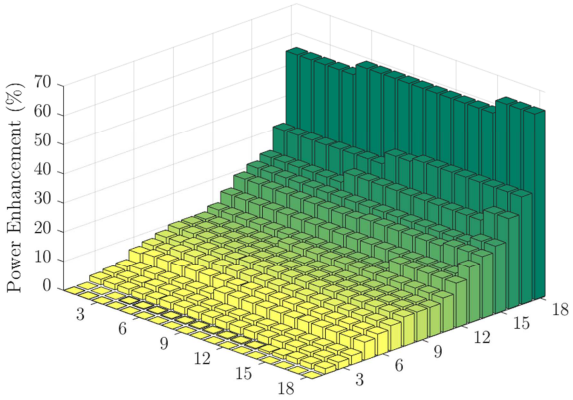

(e)

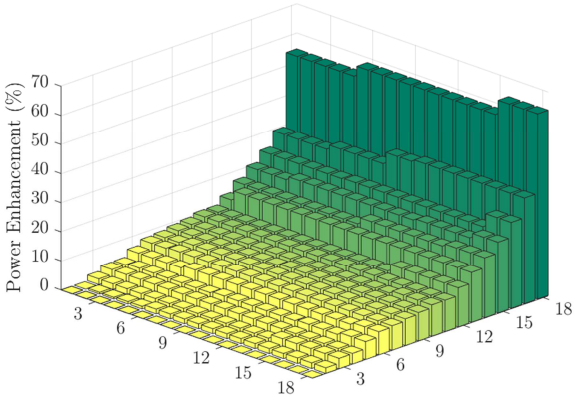

(f)

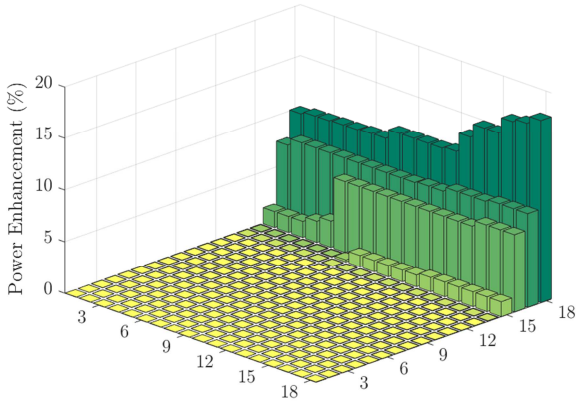

(g)

Figure 4.1: Power enhancement for all possible shading patterns of a 6×6 PV array comparing SD with (a) SP, (b) BL, (c) HC, (d) TCT, (e) SP-TCT, (f) TCT-BL, and (g) NP technique.

To provide some details about the evaluations of different shading patterns, some of these arrays which are shown in Figure 4.2 are investigated in this section and the output power with and without considering wiring losses are reported based on the simulation results. Moreover, the number of MPPs in the P-V curve of the array is evaluated.

The length of the wires to connect the modules together is selected based on the Pythagorean distance theory. Table 4.1 represents the wiring features of a 6×6 PV array. As can be seen, the minimum wiring length is for SP scheme, so it is expected that this topology has the minimum wiring losses, and the maximum one is for NP connection due to the highest wiring length among the other interconnection methods.

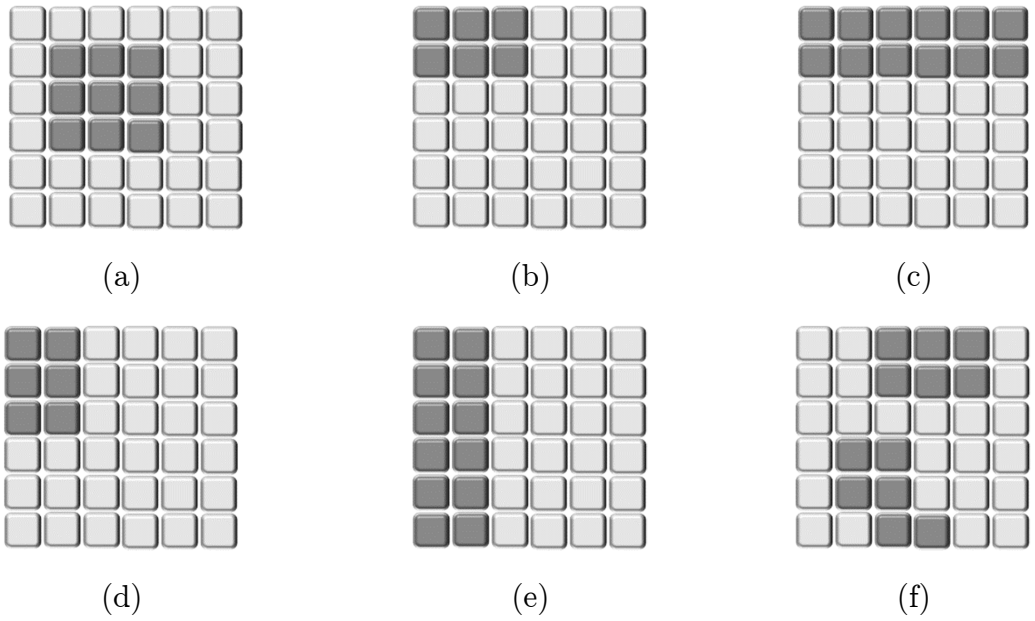

Figure 4.2: Shading patterns for a 6×6 PV array (a) Square, (b) short-horizontal (SH), (c) long-horizontal (LH) (d) short-vertical (SV), (c) long-vertical (LV), and (f) random

Table 4.1: Wiring features of a 6×6 PV array for different scheme types

Scheme Type	Wire Length (m)	Wiring Cost Increment (%)
SP	55	0
BL	79	43.6
HC	75	36.4
TCT	105	90.9
SP-TCT	79	43.6
TCT-BL	83	50.9
NP	164	198.2
SD	157	185.4

Table 4.2 shows the features of a 6×6 PV array when all panels are receiving 1000 W/m^2 illustration. In the first column, wiring losses are not considered. Thus, as there is no shading, the maximum output power of all schemes is the same. However,

in the next column, the wiring losses are considered, and NP technique shows the worst behavior among the other topologies. Figure 4.3 illustrates the P-V curve of the array with different interconnection methods.

Table 4.2: Features of a 6×6 PV array when no modules are shaded

Scheme Type	Output Power No Wiring Losses (W)	Output Power with Wiring Losses (W)	Efficiency Improvement (%)	Number of MPPs	Fill Factor
SP	12,039	12,023	0.14	1	0.783
BL	12,039	12,023	0.14	1	0.783
TCT	12,039	12,023	0.14	1	0.783
HC	12,039	12,023	0.14	1	0.783
SP-TCT	12,039	12,023	0.14	1	0.783
TCT-BL	12,039	12,023	0.14	1	0.783
NP	12,039	12,006	0	1	0.776
SD	12,039	12,011	0.04	1	0.778

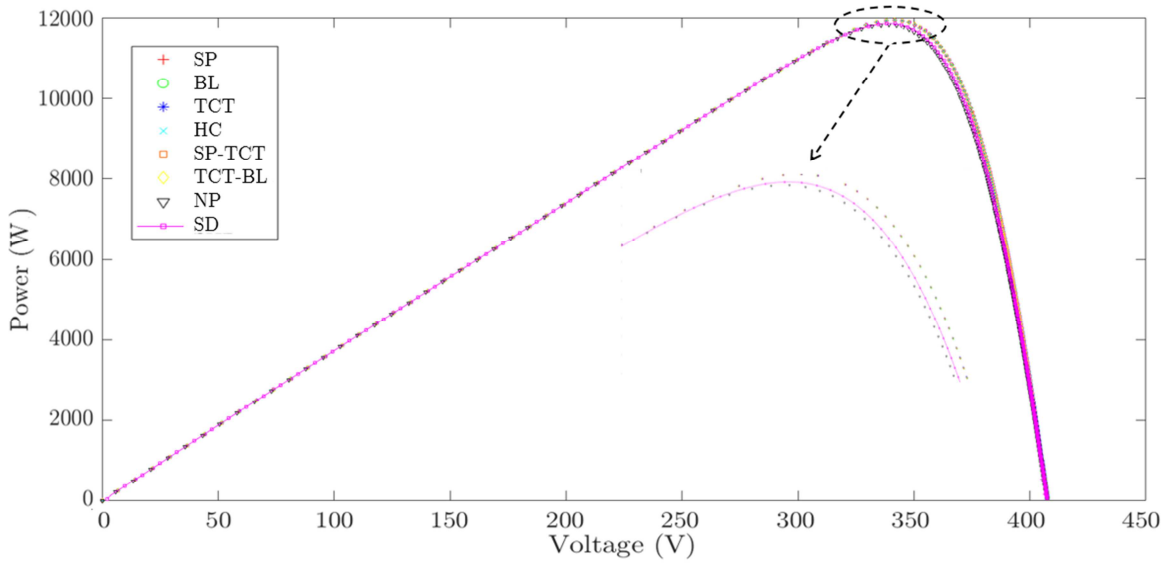

Figure 4.3: P-V curve of a 6×6 PV array with different schemes under no shading

Table 4.3 shows the features of the array under Square shading pattern which results in the power reduction of a string; consequently, the output power of the whole array is reduced. As can be seen, SP connection is the lowest efficient scheme, whereas SD generates the highest amount of power. The P-V curve of the array under this shading pattern with different interconnection methods is shown in Figure 4.4.

Table 4.3: Features of a 6×6 PV array under Square shading pattern

Scheme Type	Output Power No Wiring Losses (W)	Output Power with Wiring Losses (W)	Efficiency Improvement (%)	Number of MPPs	Fill Factor
SP	9,195	9,185	0	3	0.603
BL	9,380	9,370	2.01	3	0.615
TCT	9,733	9,723	5.86	3	0.638
HC	9,369	9,359	1.89	3	0.614
SP-TCT	9,578	9,570	4.19	3	0.628
TCT-BL	9,615	9,605	4.57	3	0.63
NP	10,405	10,383	13.04	3	0.725
SD	10,631	10,611	15.53	2	0.742

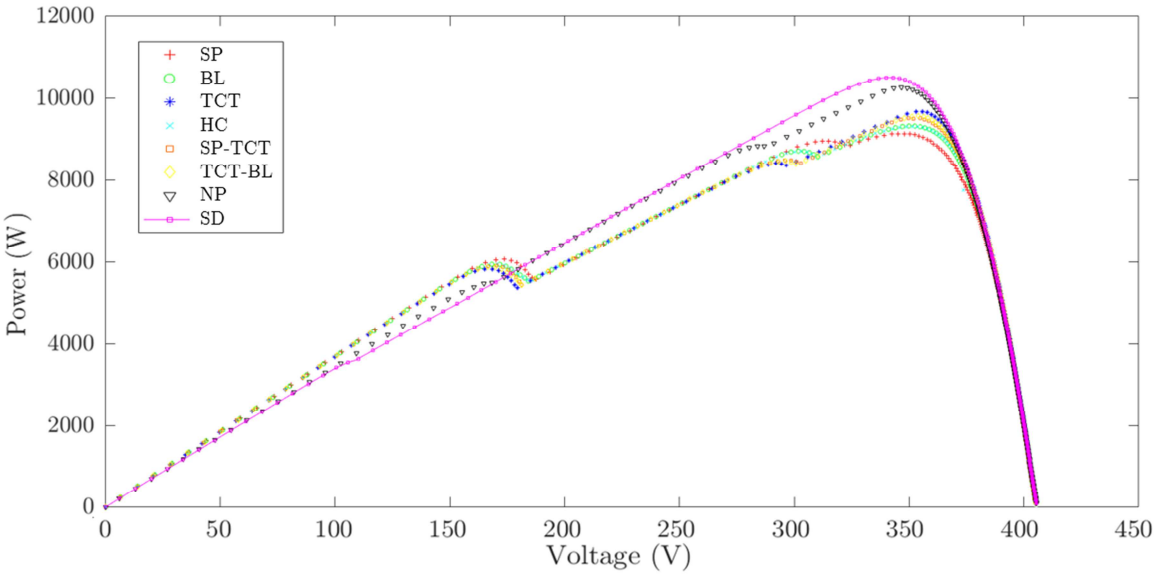

Figure 4.4: P-V curve of a 6×6 PV array with different schemes under Square shading

The features of simulating SH shading pattern on six panels belonged to three strings, shown in Figure 4.2 (b), is represented in Table 4.4. Under this condition, HC has the lowest efficiency; however, SD shows a considerable efficiency improvement by 27.27% compared with HC. The P-V curve of the array with different configuration methods, shown in Figure 4.5, provides more details about the output power considering wiring losses.

Table 4.4: Features of a 6×6 PV array under SH shading pattern

Scheme Type	Output Power No Wiring Losses (W)	Output Power with Wiring Losses (W)	Efficiency Improvement (%)	Number of MPPs	Fill Factor
SP	9,008	8,997	5.79	3	0.59
BL	8,845	8,834	3.87	3	0.579
TCT	8,700	8,692	2.2	3	0.57
HC	8,514	8,505	0	4	0.558
SP-TCT	8,687	8,679	2.05	3	0.57
TCT-BL	8,813	8,802	3.49	3	0.578
NP	10,844	10,733	26.2	2	0.701
SD	10,844	10,824	27.27	2	0.756

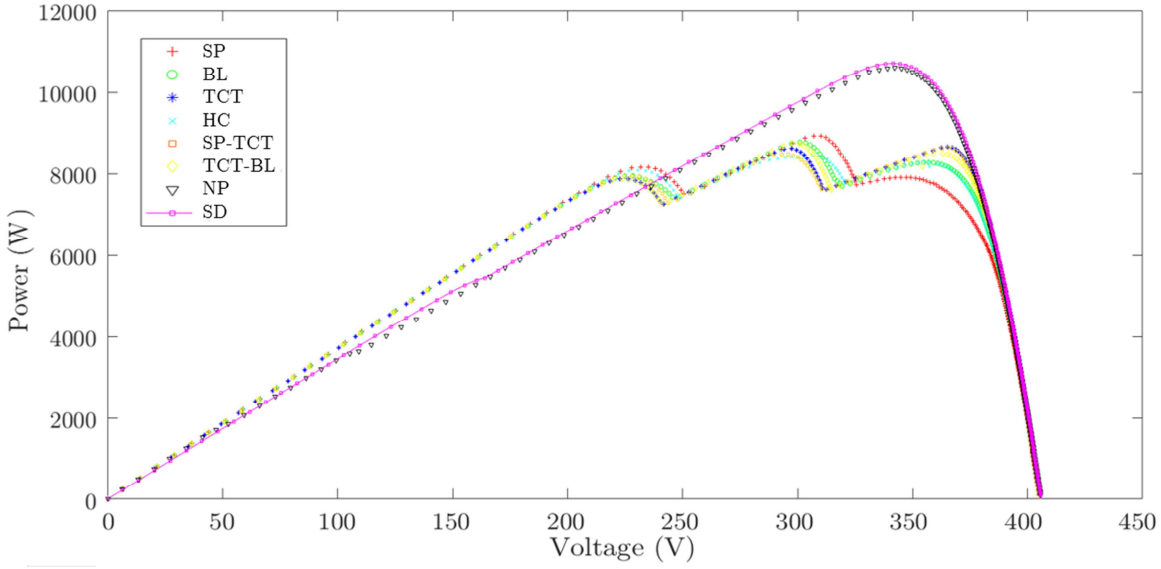

Figure 4.5: P-V curve of a 6×6 PV array with different schemes under SH shading

Table 4.5 reports the characteristic of the PV array under LH shading pattern shown in Figure 4.2 (c). The performance of SP scheme is the worst, and that of the SD is the best among the other schemes due to its capability to distribute the shade over the array. Thus, comparing the output power of SD with other methods, the generated output power can be improved by 2.84 - 23.14% under this PS which is shown in the P-V curves of Figure 4.6.

Table 4.5: Features of a 6×6 PV array under LH shading pattern

Scheme Type	Output Power No Wiring Losses (W)	Output Power with Wiring Losses (W)	Efficiency Improvement (%)	Number of MPPs	Fill Factor
SP	7,970	7,953	0	3	0.522
BL	7,970	7,953	0	3	0.522
TCT	7,970	7,953	0	3	0.522
HC	7,970	7,953	0	3	0.522
SP-TCT	7,970	7,953	0	3	0.522
TCT-BL	7,970	7,953	0	3	0.522
NP	9,813	9,523	19.74	2	0.708
SD	9,813	9,793	23.14	1	0.785

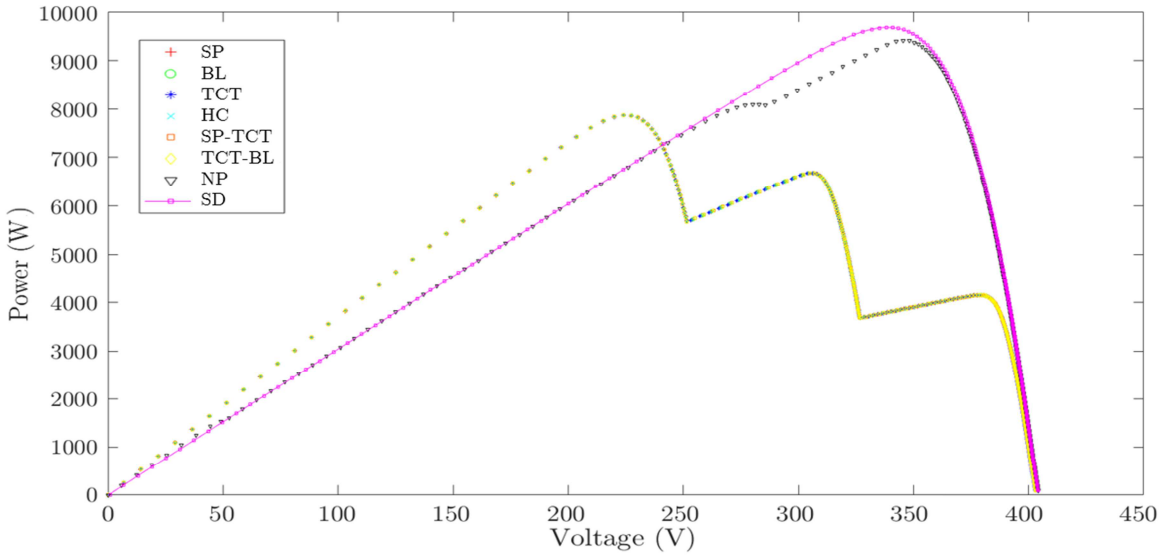

Figure 4.6: P-V curve of a 6×6 PV array with different schemes under LH shading

The specifications of simulating SV pattern, shown in Figure 4.2 (d), are provided in Table 4.6. In this case, the output current of the shaded strings are reduced which leads to a reduction in the output power. Comparing Table 4.4 and 4.6, it is clear that if PS happens on a row, the output power is decreased more than if it happens on a string. SD connection method is again performing better than the other methods as can be seen in Figure 4.7.

Table 4.6: Features of a 6×6 PV array under SV shading pattern

Scheme Type	Output Power No Wiring Losses (W)	Output Power with Wiring Losses (W)	Efficiency Improvement (%)	Number of MPPs	Fill Factor
SP	9,921	9,909	0	2	0.789
BL	10,076	10,065	1.57	2	0.789
TCT	10,271	10,260	3.54	2	0.789
HC	10,080	10,071	1.64	2	0.789
SP-TCT	10,271	10,260	3.54	2	0.789
TCT-BL	10,171	10,160	2.53	2	0.789
NP	10,360	10,338	4.33	4	0.785
SD	10,475	10,456	5.52	2	0.791

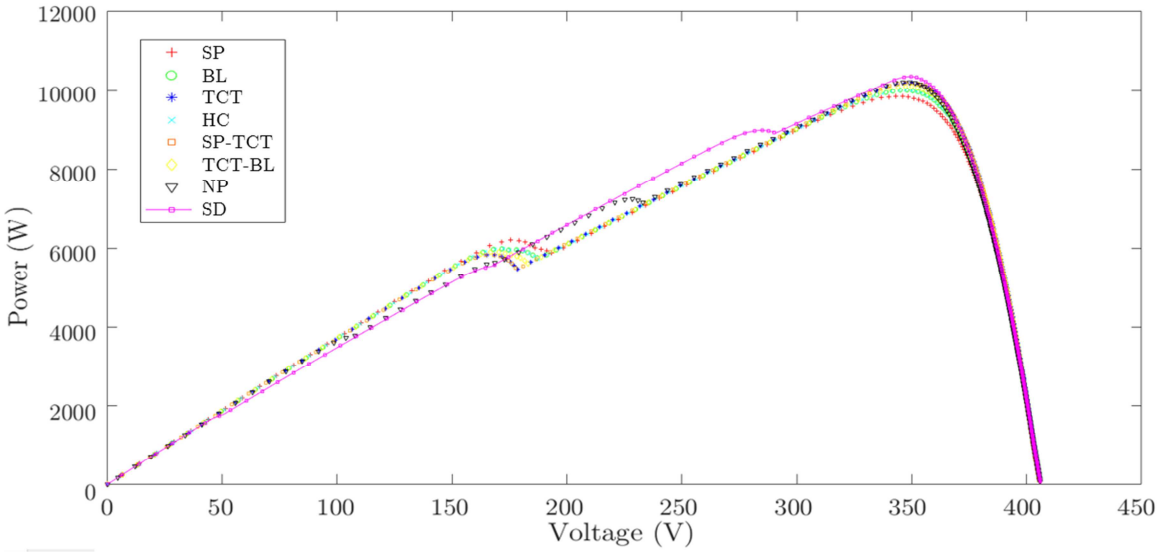

Figure 4.7: P-V curve of a 6×6 PV array with different schemes under SV shading

Table 4.7 illustrates the characteristics of the PV array under LV PS pattern represented in Figure 4.2 (e). As all modules in a string are shaded, if wiring losses are not considered, the maximum output power is the same for all scheme types. However, as the length of wires is longer in NP and SD connections, their output power is slightly lower. As can be seen in the table and Figure 4.8 this amount is low enough to be neglected.

Table 4.7: Features of a 6×6 PV array under LV shading pattern

Scheme Type	Output Power No Wiring Losses (W)	Output Power with Wiring Losses (W)	Efficiency Improvement (%)	Number of MPPs	Fill Factor
SP	9,813	9,801	0.07	1	0.789
BL	9,813	9,801	0.07	1	0.789
TCT	9,813	9,801	0.07	1	0.789
HC	9,813	9,801	0.07	1	0.789
SP-TCT	9,813	9,801	0.07	1	0.789
TCT-BL	9,813	9,801	0.07	1	0.789
NP	9,813	9,794	0	1	0.785
SD	9,813	9,797	0.03	1	0.791

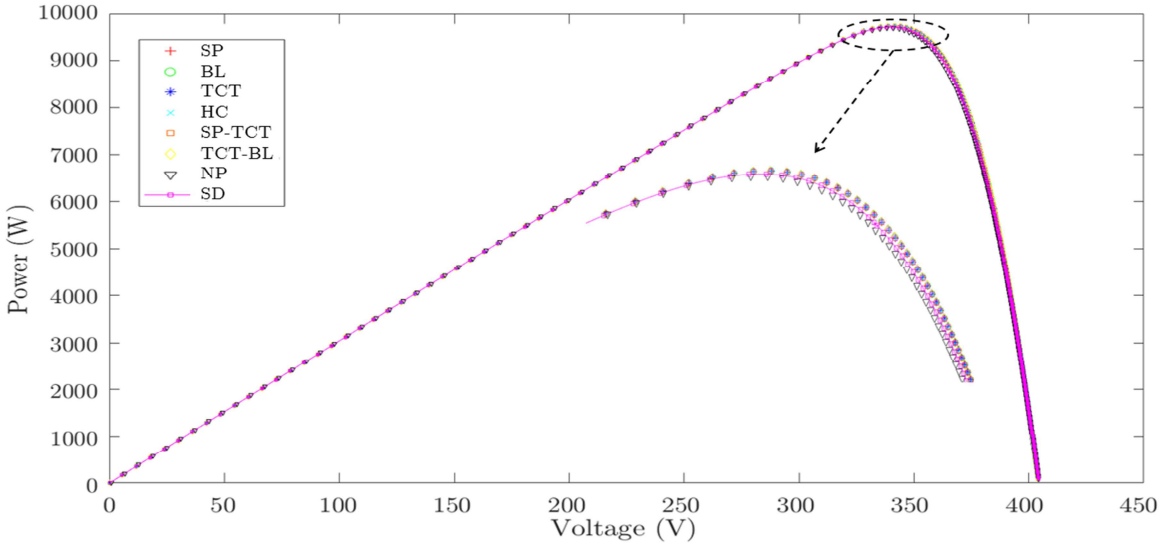

Figure 4.8: P-V curve of a 6×6 PV array with different schemes under LV shading

It is necessary to examine the efficiency of the different schemes under random shading pattern. Thus, the features of the PV array under this PS, depicted in Figure 4.2 (f), are shown in Table 4.8. SP has the lowest efficiency, whereas the performance of SD is better than other methods. Also, as illustrated in Figure 4.9, SD method shows only 2 MPPs comparing with 4 and 5 MPPs that the other schemes represent.

Table 4.8: Features of a 6×6 PV array under random shading pattern

Scheme Type	Output Power No Wiring Losses (W)	Output Power with Wiring Losses (W)	Efficiency Improvement (%)	Number of MPPs	Fill Factor
SP	7,251	7,239	0	5	0.479
BL	8,546	8,537	17.93	4	0.565
TCT	8,948	8,939	23.48	4	0.592
HC	7,497	7,472	3.2	5	0.495
SP-TCT	8,773	8,764	21.07	4	0.58
TCT-BL	8,762	8,753	20.91	4	0.579
NP	9,083	9,037	24.84	5	0.64
SD	9,659	9,643	33.21	2	0.736

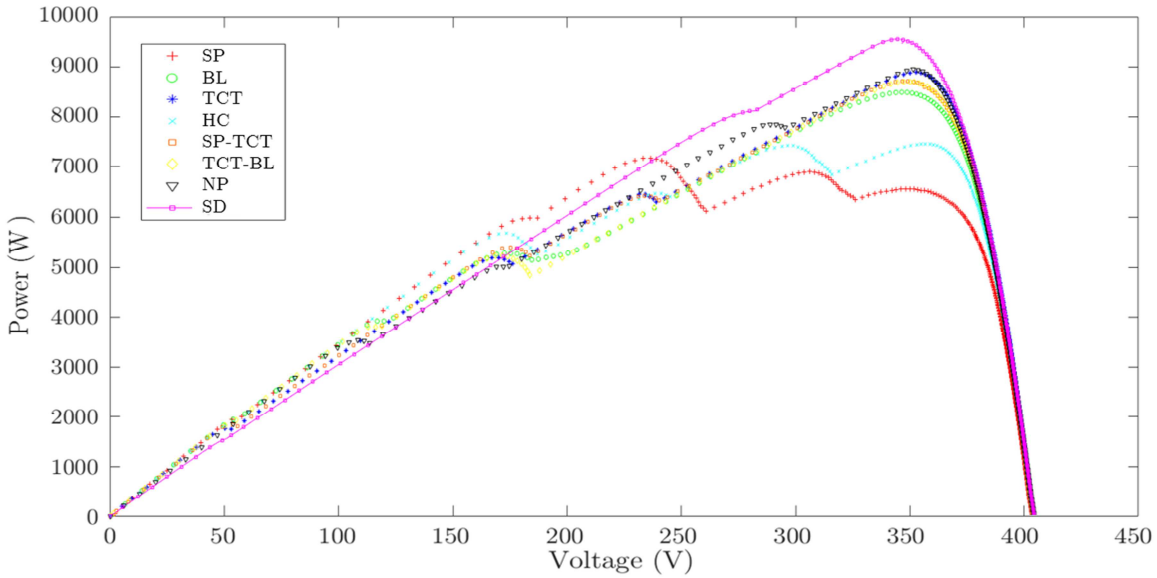

Figure 4.9: P-V curve of a 6×6 PV array with different schemes under random shading

Comparing the tables and P-V curves in this section, SD method is a better scheme by reducing the losses due to mismatch conditions. The second efficient method is NP which has a slightly higher amount of wiring compared to SD. TCT, TCT-BL and SP-TCT are the next most efficient connection types which have lower wiring requirement compared with SD and NP schemes. SP, HC and BL topologies generate the lowest amount of power; however, these schemes reduce the cost of installation and maintenance due to less filed wiring.

- **9×9 PV Array**

In this section, a 9×9 PV array is examined under 1600 different shading patterns to evaluate the PE% of SD shade distribution method compared with TCT, Su Do Ku, and MS. It should be noted that NP technique is not considered here due to its array size incompatibility with this case study. Based on the simulation results shown in the plots of Figure 4.10, SD generates up to 44.8%, 8.4%, and 7.4% more power than TCT, Su Do Ku and MS, respectively. This power enhancement is due to the better capability of SD shade distribution technique in distributing the shade and lower wiring losses.

Additionally, the effects of different shading patterns, shown is Figure 4.11, on the output power of a 9×9 PV array with and without considering wiring losses and the number of MPPs are evaluated. Based on the simulation results, the short circuit current of the PV array is 54 amp, therefore, a 6 AWG wire which can tolerate 55 amp current and has the wiring resistance of 1.296 ohm per 1000 m is selected for this array size. Table 4.9 represents the wiring characteristics of a 9×9 PV array with MS and SP methods having the highest and lowest wiring cost, respectively.

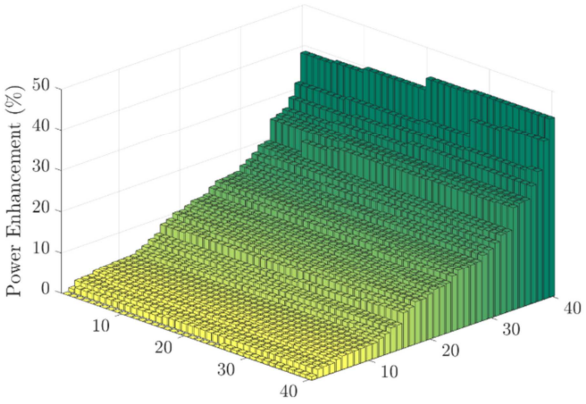
Power Enhancement (%)
0
10
20
30
40
50
10
20
30
40

(a)

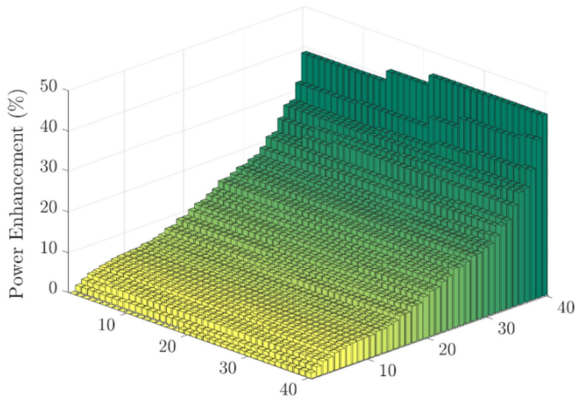
Power Enhancement (%)
0
10
20
30
40
50
10
20
30
40

(b)

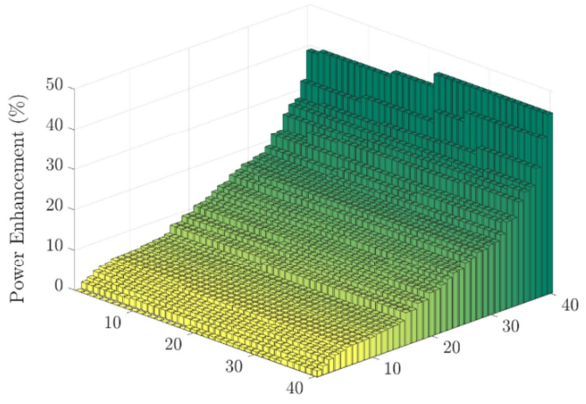
Power Enhancement (%)
0
10
20
30
40
50
10
20
30
40

(c)

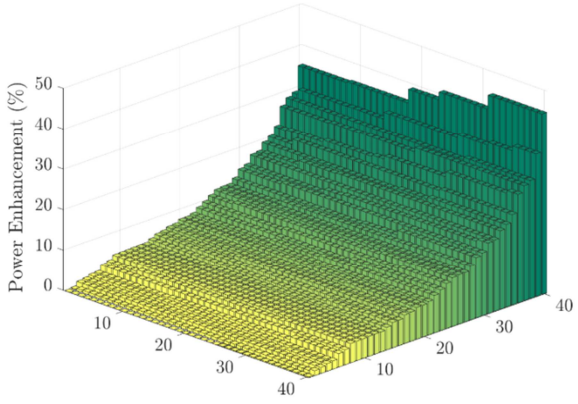
Power Enhancement (%)
0
10
20
30
40
50
10
20
30
40

(d)

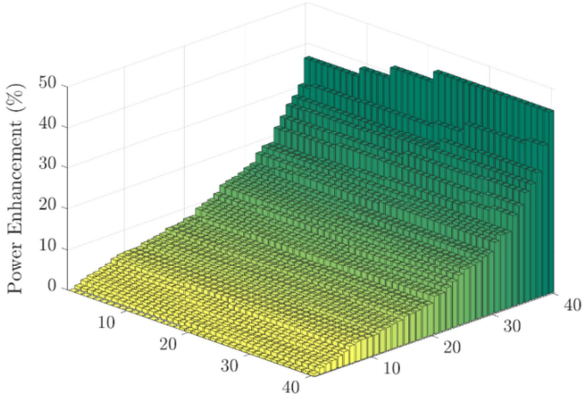
Power Enhancement (%)
0
10
20
30
40
50
10
20
30
40

(e)

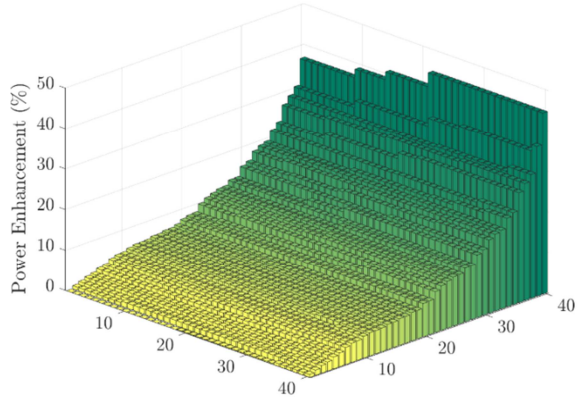
Power Enhancement (%)
0
10
20
30
40
50
10
20
30
40

(f)

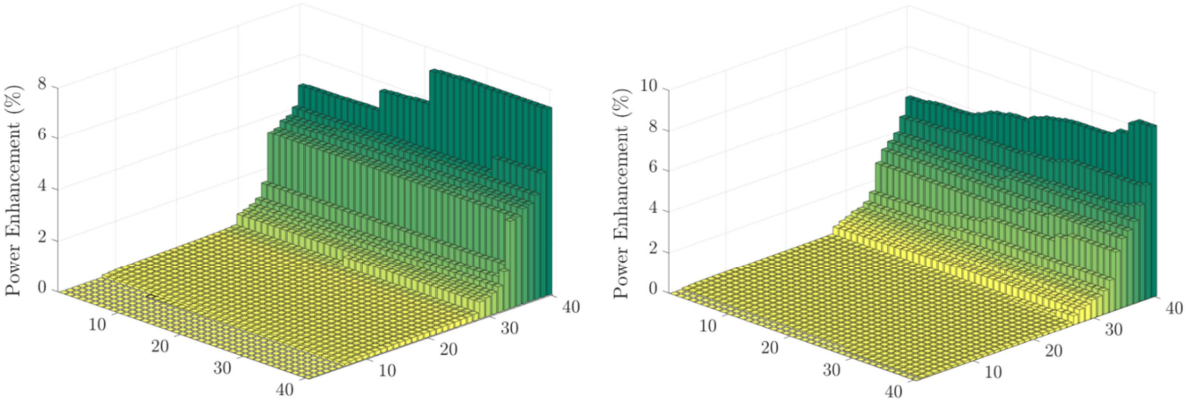

(g) (h)

Figure 4.10: Power enhancement for all possible shading patterns of a 9×9 PV array comparing SD with (a) SP, (b) BL, (c) HC, (d) TCT, (e) SP-TCT, (f) TCT-BL, (g) MS, and (h) Su Do Ku

Table 4.9: Wiring features of a 9×9 PV array for different scheme types

Scheme Type	Wire Length (m)	Wiring Cost Increment (%)
SP	112	0
BL	176	57
TCT	240	114
HC	176	57
SP-TCT	176	57
TCT-BL	208	86
MS	762	580
Su Do Ku	461	312
SD	407	263

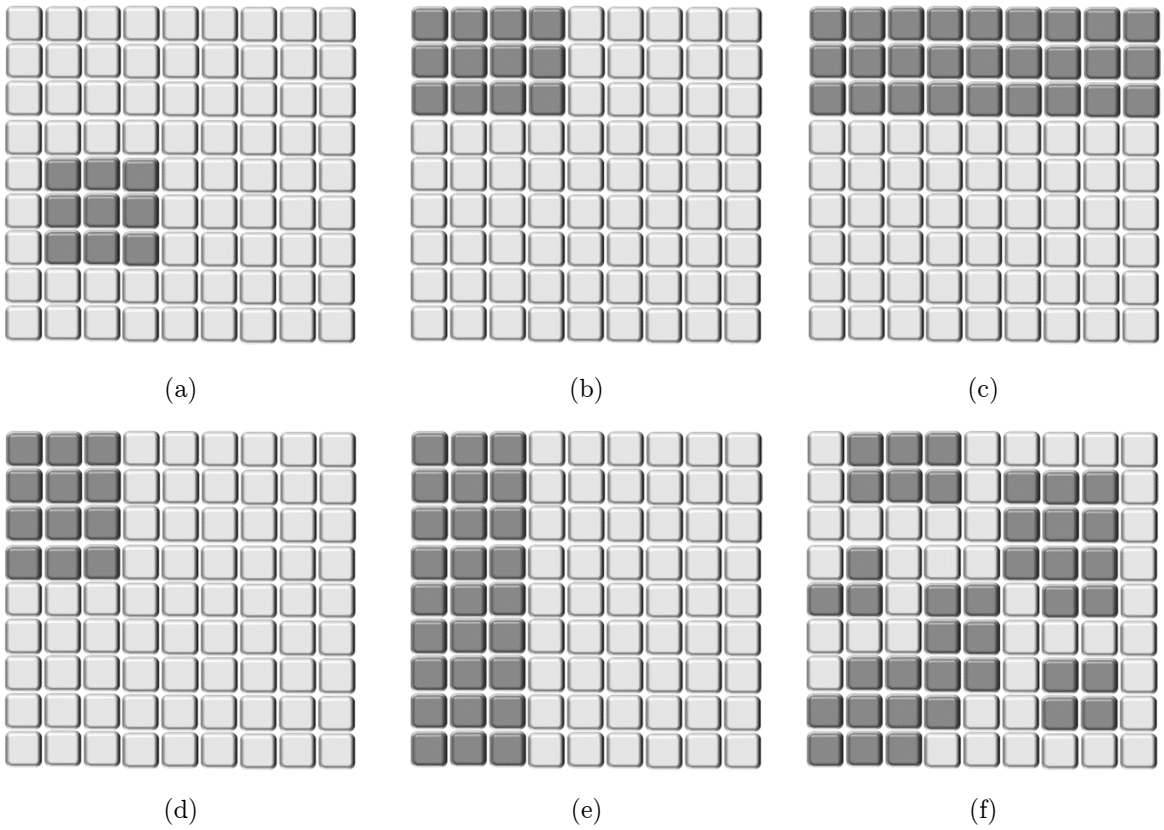

(a) (b) (c)

(d) (e) (f)

Figure 4.11: Shading patterns for a 9×9 PV array (a) Square, (b) SH, (c) LH, (d) SV, (c) LV, and (f) random

Table 4.10 demonstrates the specifications of the array under no shading. As can be seen in the P-V curve of this array, shown in Figure 4.12, if wiring losses are considered, due to higher wiring length of the shade distributing methods, MS, Su Do Ku and SD have higher wiring losses and lower performance.

Table 4.10: Features of a 9×9 PV array when no modules are shaded

Scheme Type	Output Power No Wiring Losses (W)	Output Power with Wiring Losses (W)	Efficiency Improvement (%)	Number of MPPs	Fill Factor
SP	27,088	27,055	0.35	1	0.779
BL	27,088	27,055	0.35	1	0.779
TCT	27,088	27,055	0.35	1	0.779
HC	27,088	27,055	0.35	1	0.779
SP-TCT	27,088	27,055	0.35	1	0.779
TCT-BL	27,088	27,055	0.35	1	0.779
MS	27,088	26,962	0	1	0.746
Su Do Ku	27,088	26,978	0.06	1	0.754
SD	27,088	27,018	0.21	1	0.765

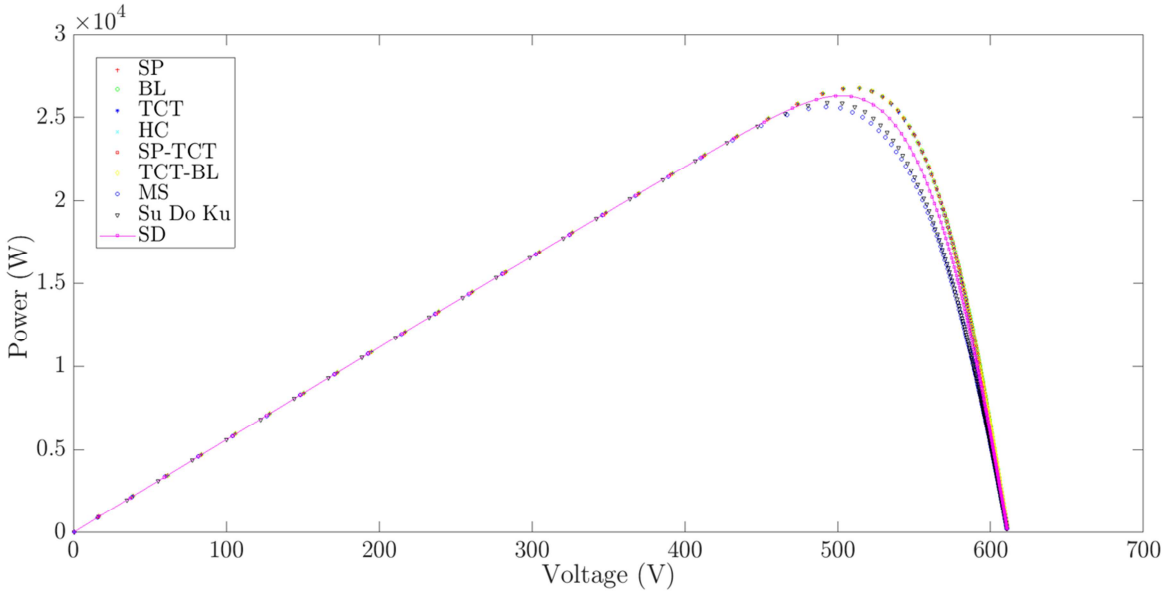

Figure 4.12: P-V curve of a 9×9 PV array with different schemes under no shading

The features and P-V curve of the array under Square shading pattern, shown in Figure 4.11 (a), is represented in Table 4.11 and Figure 4.13, respectively. Here, SP, BL and HC are the lowest efficient schemes, whereas SD and MS generate the highest amount of power and demonstrate only one MPP in their P-V curve.

Table 4.11: Features of a 9×9 PV array under Square shading pattern

Scheme Type	Output Power No Wiring Losses (W)	Output Power with Wiring Losses (W)	Efficiency Improvement (%)	Number of MPPs	Fill Factor
SP	23,356	23,331	0.59	2	0.675
BL	23,317	23,293	0.42	3	0.674
TCT	24,296	24,270	4.64	3	0.703
HC	23,219	23,195	0	3	0.672
SP-TCT	24,016	23,993	3.44	3	0.695
TCT-BL	24,064	24,038	3.63	3	0.696
MS	25,501	25,396	9.49	1	0.711
Su Do Ku	25,501	24,213	4.39	3	0.686
SD	25,502	25,444	9.7	1	0.727

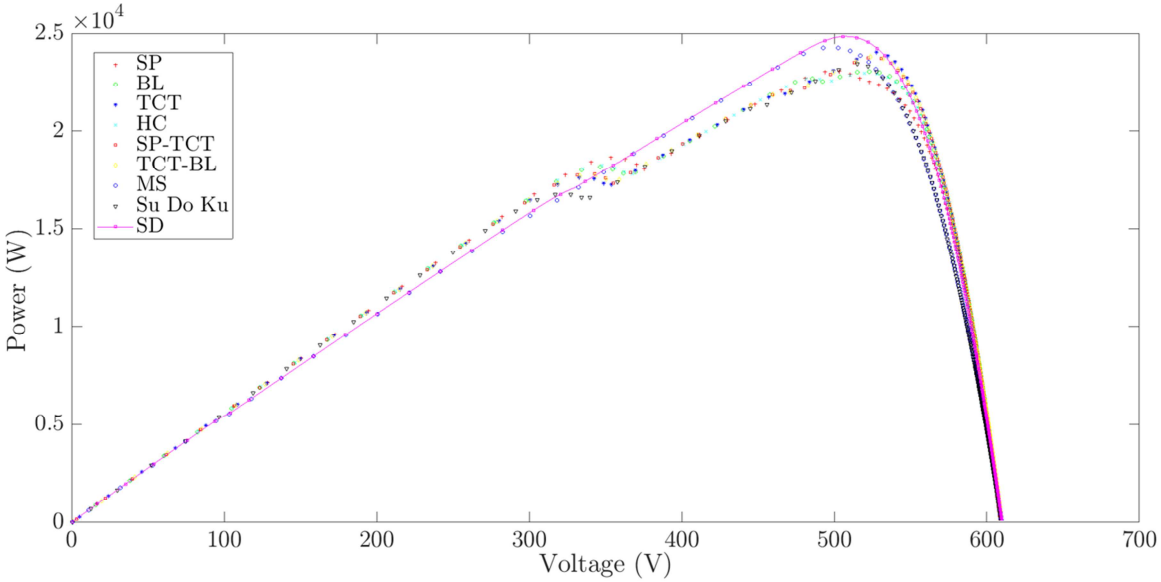

Figure 4.13: P-V curve of a 9×9 PV array with different schemes under Square shading

Table 4.12 shows the features of simulating SH shading pattern on the array, shown in Figure 4.11 (b). SD demonstrates a very good output power improvement by up to 24.88% with only one MPP compared to three MPPs of non-shade distributing methods in their P-V curve shown in Figure 4.14.

Table 4.12: Features of a 9×9 PV array under SH shading pattern

Scheme Type	Output Power No Wiring Losses (W)	Output Power with Wiring Losses (W)	Efficiency Improvement (%)	Number of MPPs	Fill Factor
SP	19,661	19,637	0.54	3	0.569
BL	19,610	19,596	0.33	3	0.569
TCT	20,479	20,462	4.77	3	0.594
HC	19,548	19,531	0	3	0.567
SP-TCT	20,269	20,250	3.68	3	0.588
TCT-BL	20,458	20,444	4.68	3	0.594
MS	21,268	23,891	22.32	1	0.679
Su Do Ku	24,160	24,082	23.3	1	0.716
SD	24,444	24,391	24.88	1	0.735

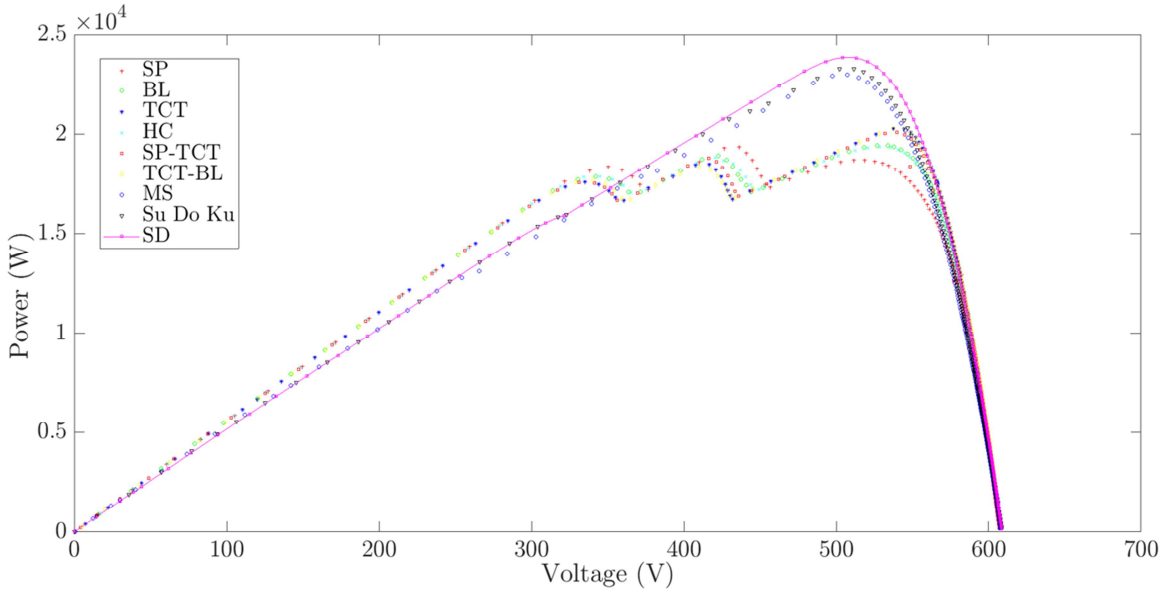

Figure 4.14 P-V curve of a 9×9 PV array with different schemes under SH shading

LH shading pattern, shown in Figure 4.11 (c), is considered next and the characteristics are reported in Table 4.13 and Figure 4.15. Under this PS, MS, Su Do Ku and SD generate around 3.6 KW more power compared to non-reconfigured interconnection methods with only one MPP.

Table 4.13: Features of a 9×9 PV array under LH shading pattern

Scheme Type	Output Power No Wiring Losses (W)	Output Power with Wiring Losses (W)	Efficiency Improvement (%)	Number of MPPs	Fill Factor
SP	17,932	17,899	0	3	0.52
BL	17,932	17,899	0	3	0.52
TCT	17,932	17,899	0	3	0.52
HC	17,932	17,899	0	3	0.52
SP-TCT	17,932	17,899	0	3	0.52
TCT-BL	17,932	17,899	0	3	0.52
MS	19,217	21,549	20.39	1	0.765
Su Do Ku	21,619	21,551	20.4	1	0.768
SD	21,619	21,573	20.53	1	0.776

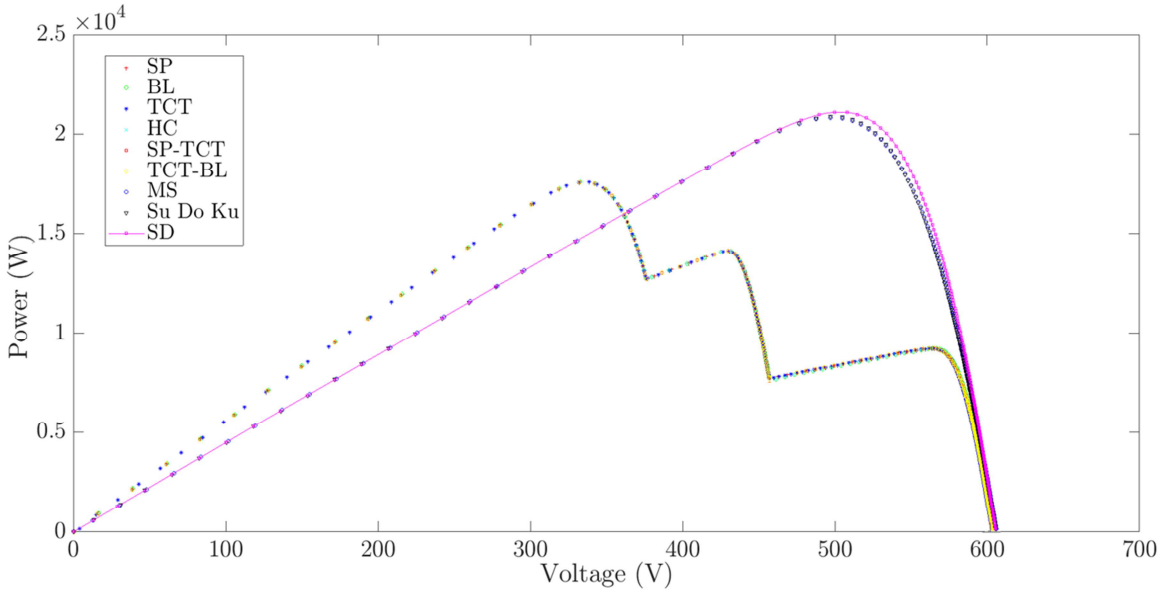

Figure 4.15: P-V curve of a 9×9 PV array with different schemes under LH shading

The specifications of simulating SV shading pattern, shown in Figure 4.11 (d), is provided in Table 4.14. MS shade distribution method outperforms the other techniques, however, SP shows the worth behaviour. Also, as can be seen in Figure 4.16, only MS and SD have one MPP in their P-V curve under this shading pattern.

Table 4.14: Features of a 9×9 PV array under SV shading pattern

Scheme Type	Output Power No Wiring Losses (W)	Output Power with Wiring Losses (W)	Efficiency Improvement (%)	Number of MPPs	Fill Factor
SP	21,859	21,837	0	2	0.634
BL	22,261	22,238	1.84	2	0.646
TCT	22,822	22,799	4.41	2	0.662
HC	22,184	22,161	1.48	2	0.643
SP-TCT	22,602	22,579	3.4	2	0.655
TCT-BL	22,824	22,799	4.41	2	0.662
MS	24,444	24,349	11.5	1	0.723
Su Do Ku	23,116	22,949	5.09	2	0.712
SD	23,984	23,933	9.6	1	0.691

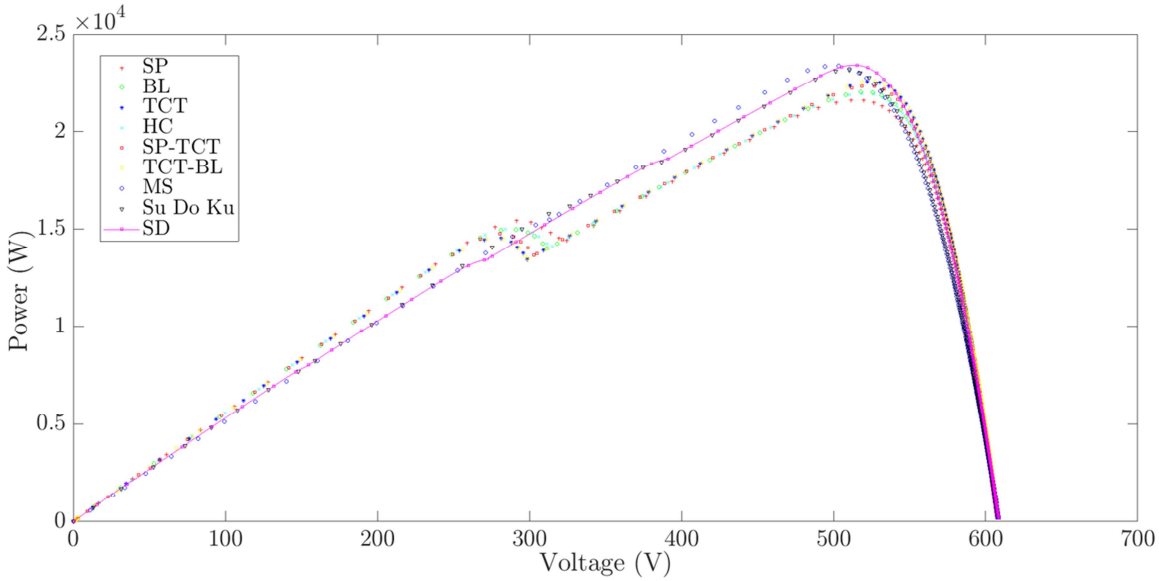

Figure 4.16: P-V curve of a 9×9 PV array with different schemes under SV shading

Table 4.15 illustrates the features of the PV array under LV shading pattern represented in Figure 4.11 (e). Similar to unshaded pattern, the output power of MS method is slightly lower due to higher wire length. Moreover, under this PS, all patterns show only one MPP in their P-V curve illustrated in Figure 4.17.

Table 4.15: Features of a 9×9 PV array under LV shading pattern

Scheme Type	Output Power No Wiring Losses (W)	Output Power with Wiring Losses (W)	Efficiency Improvement (%)	Number of MPPs	Fill Factor
SP	21,619	21,598	0.25	1	0.787
BL	21,619	21,598	0.25	1	0.787
TCT	21,619	21,598	0.25	1	0.787
HC	21,619	21,598	0.25	1	0.787
SP-TCT	21,619	21,598	0.25	1	0.787
TCT-BL	21,619	21,598	0.25	1	0.787
MS	21,619	21,544	0	1	0.763
Su Do Ku	21,619	21,558	0.07	1	0.771
SD	21,619	21,583	0.18	1	0.78

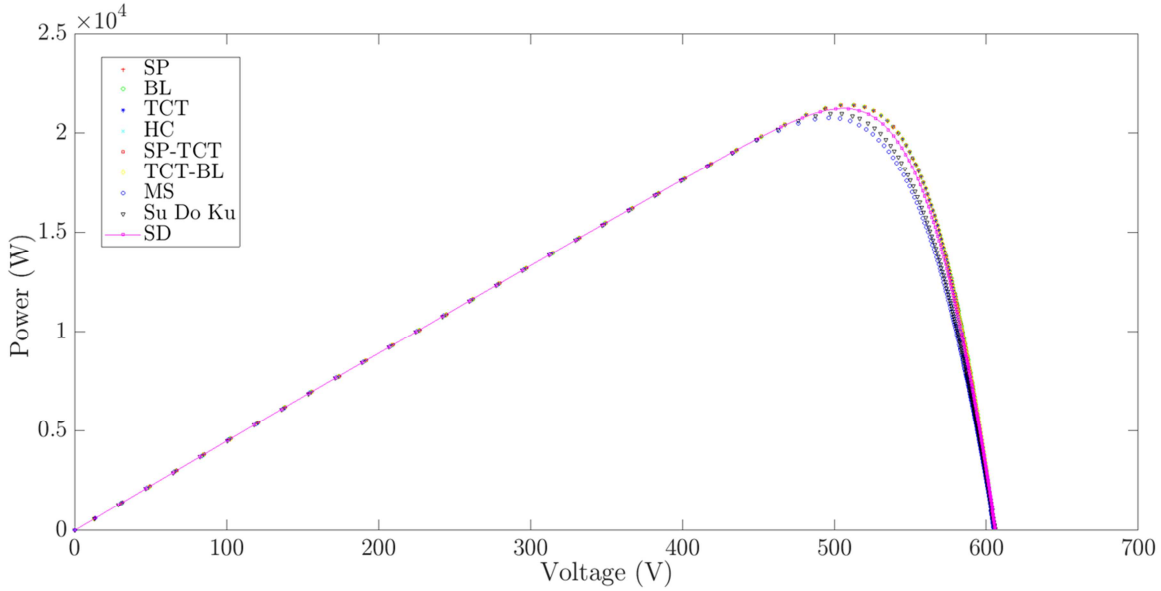

Figure 4.17: P-V curve of a 9×9 PV with different schemes under LV shading

The features of the PV array under random shading, illustrated in Figure 4.11 (f), are shown in Table 4.16 and Figure 4.18. Here, the performance of SD is well above the other methods by up to 38.66% increment in the output power with only showing two MPPs.

Table 4.16 Features of a 9×9 PV array under random shading pattern

Scheme Type	Output Power No Wiring Losses (W)	Output Power with Wiring Losses (W)	Efficiency Improvement (%)	Number of MPPs	Fill Factor
SP	13,859	13,840	0	6	0.404
BL	16,002	16,086	16.23	5	0.474
TCT	17,878	17,864	29.08	5	0.599
HC	15,483	15,464	11.73	6	0.476
SP-TCT	16,994	16,981	22.7	5	0.549
TCT-BL	17,405	17,383	25.6	6	0.562
MS	18,661	18,598	34.38	2	0.643
Su Do Ku	18,944	18,895	36.53	2	0.592
SD	19,225	19,191	38.66	2	0.616

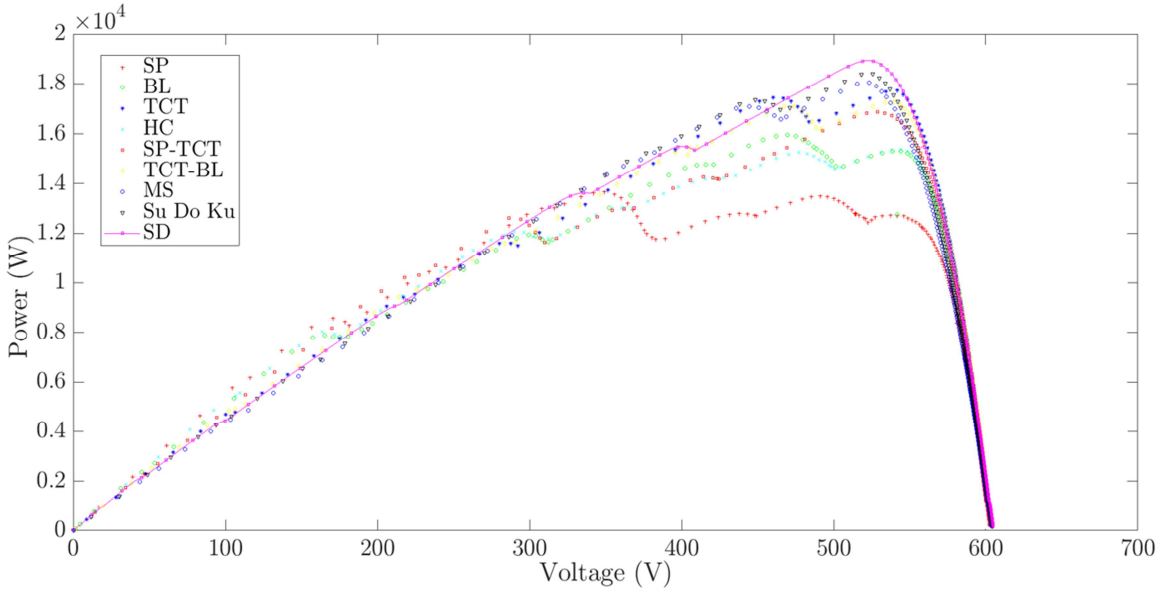

Figure 4.18: P-V curve of a 9×9 PV array with different schemes under random shading

4.2 Power Enhancement Evaluation for a Case Study During a Summer Day

A 42 KWh PV system installed on the roof of the North Vancouver Library is selected for this case study which is equipped with 120 PV panels, shown in Figure 4.19 (a). During afternoons, this plant is highly affected by PS due to its surrounding high-rises which can be seen in part (b) of the figure. The location of this PV system is -123.07 degrees west (longitude) and 49.32 degrees north (latitude) with the altitude of 260 feet.

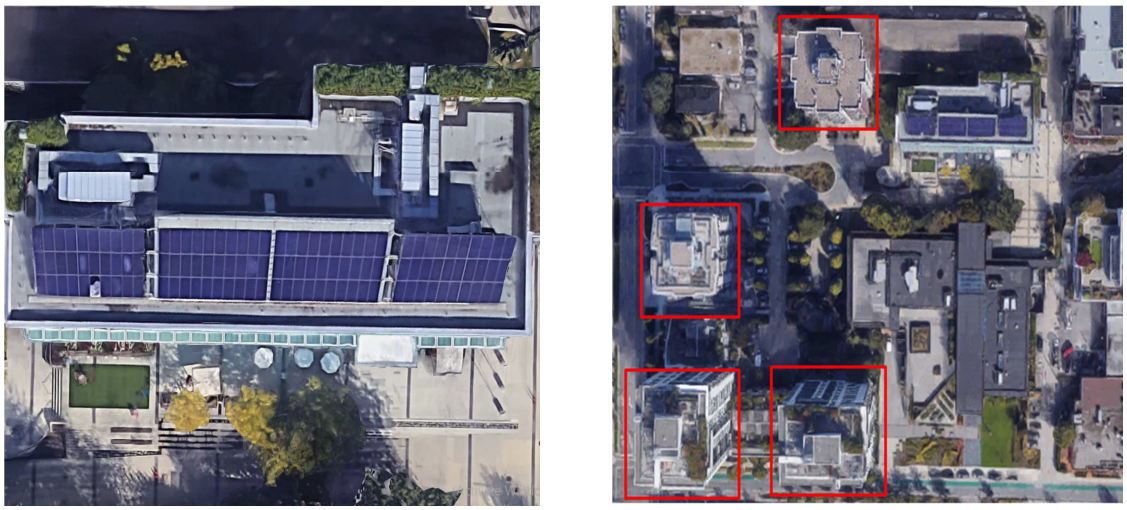

(a) (b)

Figure 4.19: (a) Roof-top PV panels of North Vancouver Library, and (b) the library surrounded by high-rises shown in red boxes shadowing the PV system.

This case study was performed on July 25th 2018 with the sunrise and sunset time of 5:35 and 21:01, respectively. Table 4.17 shows some of the shading patterns affecting this plant on that day. As shown in the table, from morning till early afternoon, no shading happened on the PV arrays; however, PS started to reduce the performance of the system afterwards until the end of the day.

Table 4.17: Some of the shading patterns based on the time of the day affecting the performance of the PV system of North Vancouver Library on July 25th 2018

Time	Shade Pattern
6-13:30	
13:30-14	
14-14:30	
14:30-15	
15-15:30	
15:30-16	
16-16:30	
16:30-17	
17-17:30	
17:30-18	
18-18:30	
18:30-19	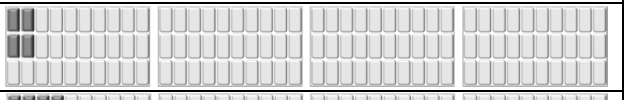
19-19:30	
19:30-20	
20-20:30	
20:30-21	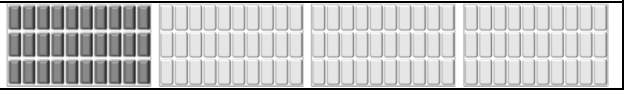

Figure 4.20 represents the power generated by this system based on the time of the day for TCT scheme and SD shade distribution method. It should be mentioned that among conventional configurations only TCT is selected for this experiment as it has the highest capability in distributing the shade. Also, the other previously mentioned shade distribution strategies are not considered for this case study due to their incompatibility with the array size of this plant. As can be seen in the figure, when PS happens, SD has a better capability in generating more power. In this research, on average, SD technique was able to generate 1.1KW in each hour more power during the operation time of the system compared to TCT interconnection configuration.

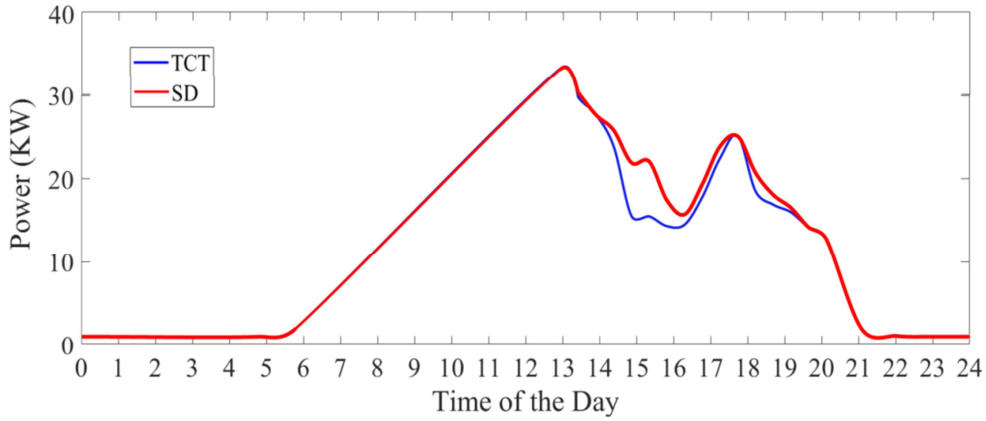

Figure 4.20: Comparison between the amount of power generated by North Vancouver library's PV plant based on the time of the day for TCT scheme and SD method.

4.3 Summary

In this chapter, to evaluate the operation of the proposed shade distribution method, all of the possible shading patterns are considered for conventional interconnection schemes and the recently emerged shade distribution techniques; and the maximum

power provided by each scheme was recorded by MATLAB/Simulink. Based on the simulation results, SD method performs better than the other schemes by reducing the losses due to mismatch condition of a partially shaded PV array specifically when shading happens in one or more rows of the array. This technique improves the efficiency of the PV panels by up to 63.7% under PS compared with other configurations. Moreover, for both 6×6 and 9×9 PV arrays eight shading pattern were selected to show the P-V curve of the array under different shading patterns. Simulation results show a considerable reduction in the number of LPs in the P-V curve of SD shade distribution technique compared with TCT interconnection due to shade distribution leading to less possibility of turning on the bypass diode. Additionally, as SD has a better capability of dispensing the shade compared to NP, MS, and Su Do Ku methods, there are less LPs in the P-V curve of this proposed technique compared to the explained recently emerged shade distribution strategies.

Chapter 5

Wiring Cost Payback

Although wiring expenses of shade distribution techniques are higher, the payback duration (PD) for this overhead cost can be short due to more power generation. Here, five case studies for a 6×6 and 9×9 PV array are explained to show the amount of time required for paying back the overhead costs of the wiring. Figure 5.1 and 5.2 illustrate the case studies for the 6×6 and 9×9 PV array, respectively. In this case studies, the location of the installed panels is considered to be in Hamilton, Ontario with the average amount of sunshine about 2111 hours per year. As can be seen in the figure, each case study is divided into four equal periods of different shading patterns. It should be mentioned that the shaded panels, shown in dark grey, receive 30% illumination of the unshaded ones.

The wiring cost of a 6 AWG and 8 AWG hook up wire which is appropriate for use in solar power applications that require 600-2,000 V rating is around 1.67 CAD and 1.15 CAD per meter, respectively. It should be mentioned that as of January 2017, Independent Electricity System Operator (IESO) of Canada pays 0.223 CAD per KWh for a 10-100 KW rooftop solar project [54].

Table 5.1 and 5.2 represent the PD for different configurations compared with SP scheme which requires the minimum amount of wiring. It should be noted that in the table "Never" means that under that specific shading pattern SP is generating

more power than the interconnection method under study, therefore, the overhead wiring costs is non-returnable.

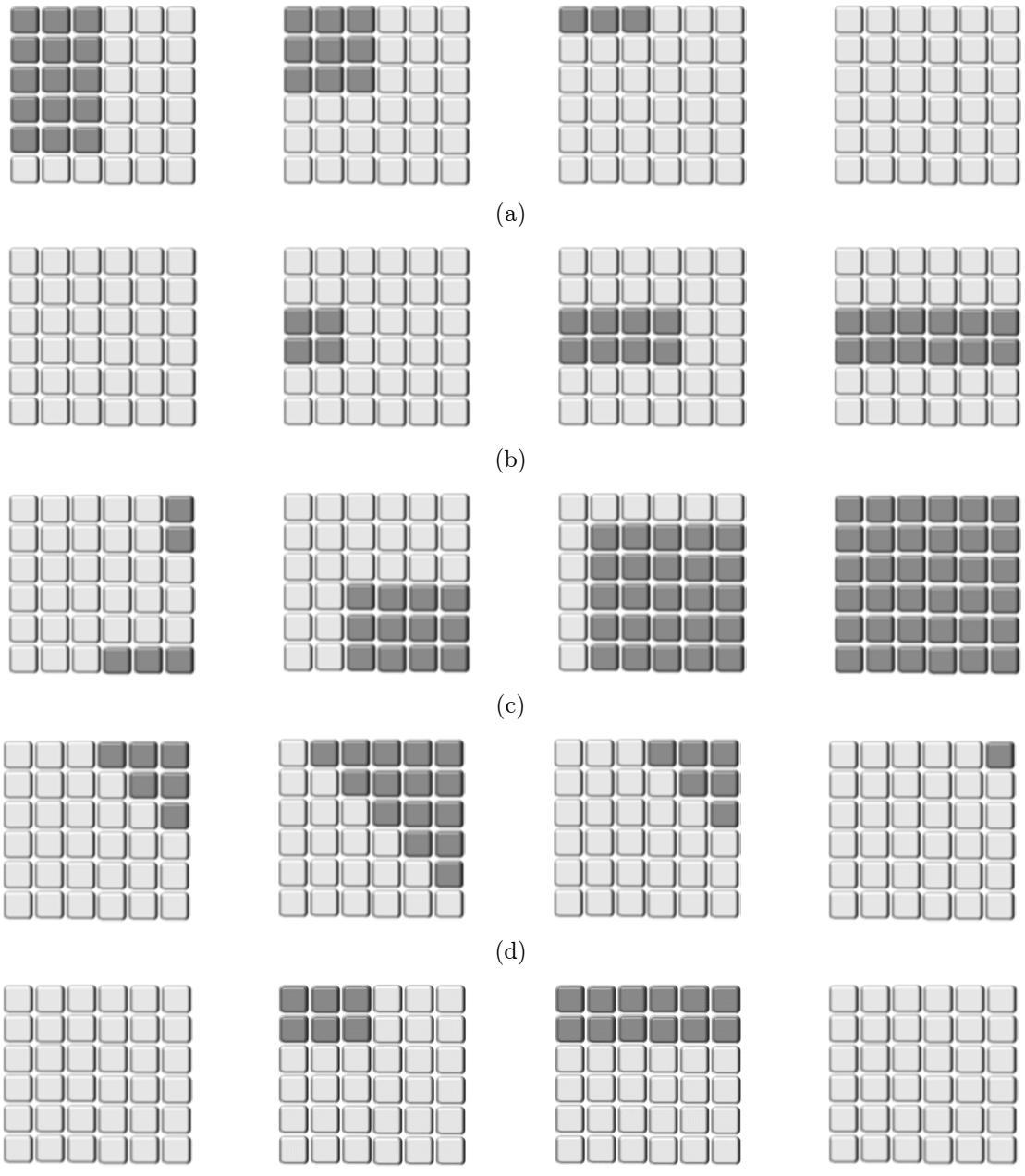

Figure 5.1: Case studies for a 6×6 PV array to evaluate the PD of overhead wiring cost (a) case study 1, (b) case study 2, (c) case study 3, (d) case study 4, and (e) case study 5.

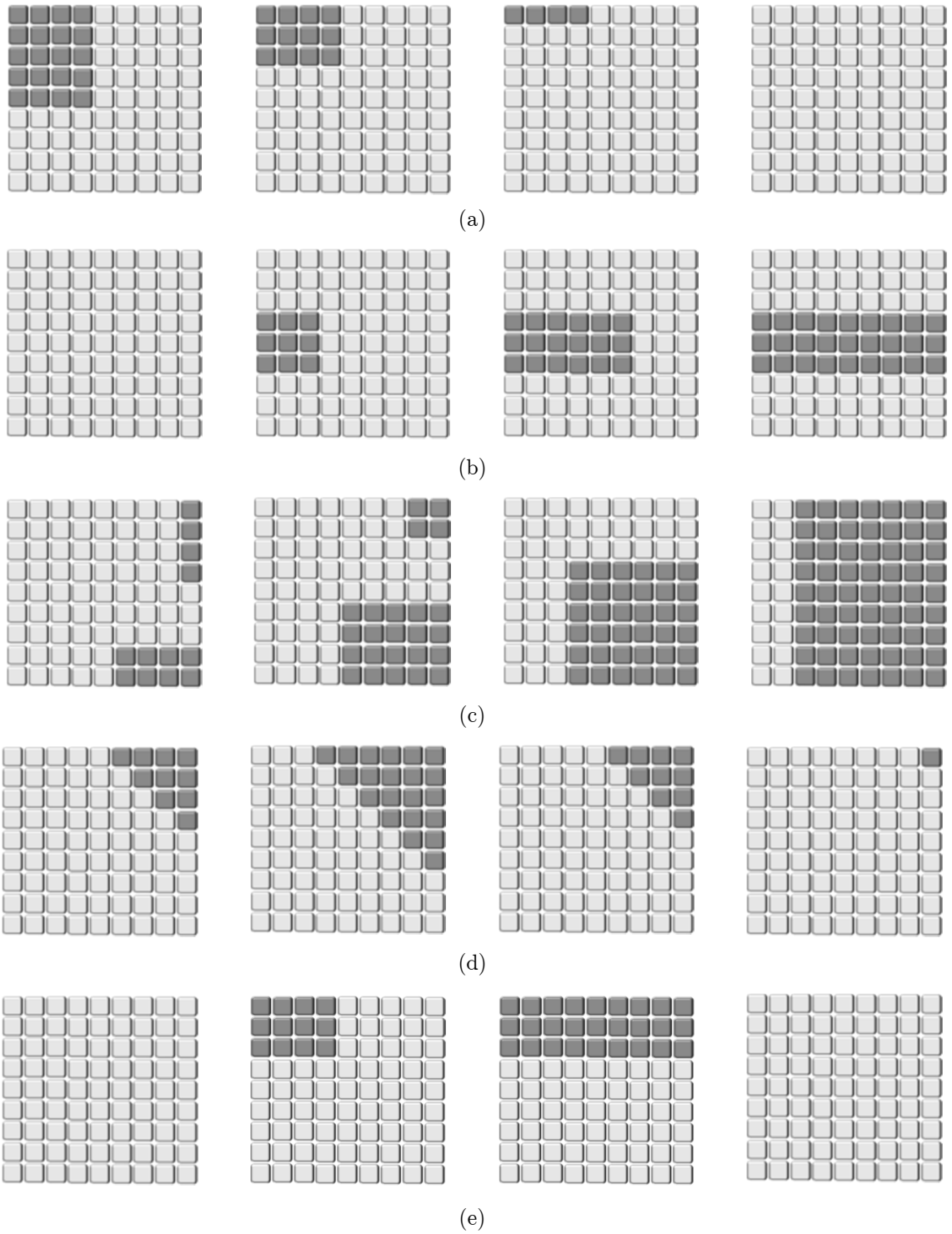

Figure 5.2: Case studies for a 9×9 PV array to evaluate the PD of overhead wiring cost (a) case study 1, (b) case study 2, (c) case study 3, (d) case study 4, and (e) case study 5.

Table 5.1: PD of five case studies shown in Figure 5.1 on a 6×6 PV array comparing different interconnection schemes with SP

Scheme Type	PD for Case Study 1 (days)	PD for Case Study 2 (days)	PD for Case Study 3 (days)	PD for Case Study 4 (days)	PD for Case Study 5 (days)
BL	Never	1,189	Never	117	Never
TCT	1,248	421	585	116	807
HC	Never	1,251	2,853	158	Never
SP-TCT	599	437	501	64	Never
TCT-BL	Never	235	379	91	Never
NP	154	112	108	63	119
SD	143	84	101	58	100

Table 5.2: PD of five case studies shown in Figure 5.2 on a 9×9 PV array comparing different interconnection schemes with SP

Scheme Type	PD for Case Study 1 (days)	PD for Case Study 2 (days)	PD for Case Study 3 (days)	PD for Case Study 4 (days)	PD for Case Study 5 (days)
BL	157	184	212	155	Never
TCT	Never	Never	Never	Never	804
HC	169	171	185	169	Never
SP-TCT	189	195	182	188	541
TCT-BL	341	365	384	338	617
MS	1,233	2,755	5,197	1,180	437
Su Do Ku	650	618	1,080	652	228
SD	514	499	388	497	166

As reported in the tables, the system can pay for the increased wiring cost of SD faster than that of the other shade distribution methods by generating more power. In fact, the PD for this overhead cost is less than two years by more power generation. Therefore, as the period of the operation of PV panels is nearly 25 years [18], the benefits of reconfiguring the panels based on SD strategy is considerably higher than the other configuration methods in particularly non-reconfigured schemes.

Chapter 6

Conclusion

6.1 Summary

Since Photovoltaic (PV) energy is expensive and precious, the need for an efficient system to transfer this power to the suppliers is essential. However, Partial Shading (PS) has a considerable effect on the performance of PV systems. When some of the panels in an array are under PS, different output power levels are generated by the panels within the same array. As the shaded panels are electrically connected to unshaded ones and the same amount of power is not generated by all of them, shaded panels absorb the power of unshaded panels. Thus, this absorption of the power causes energy losses and hot spot problems. The amount of power loss nonlinearly depends on the shade pattern, array interconnection scheme and the location of shaded modules in the array. It should be noted that if the shaded modules are located in a row, the mismatch conditions critically reduces the performance of a PV array.

This thesis introduces a fixed shade distribution method to reduce the power losses due to PS. The main six advantages of this shade distribution technique are: 1) distributing the shade over the entire array, 2) minimally relocating the PV panels inside an array which reduces the wiring length compared to the other existing shade distribution methods, 3) considerable reduction in the number of Local Peaks (LPs) in the Power-Voltage (P-V) curve of the array compared to conventional interconnection

schemes and the other shade distribution strategies, 4) less complex Maximum Power Point Tracking (MPPT) controller, 5) low cost, and 6) maintenance free.

6.2 Future Work

As the shadows of obstacles are usually fixed, a modified strategy can be proposed to combine SP for the unshaded parts of a PV array and SD for the shaded parts in order to reduce wiring costs and losses. Additionally, the original contribution of this thesis only considers the variations of the illustration level on the PV panels. By expanding this technique to include the fluctuations in the temperature of the panels, more reliable results can be obtained before field installations. Moreover, a novel bus-bar can be proposed to reduce the efforts of wiring while keeping the costs and losses minimized. Also, simulation results of this thesis represent this fact that the proposed technique limits the amount of fill factor between 0.6 and 0.8. Therefore, a new MPPT method can be introduced to only search for the MPP within that limit which further improves the efficiency of the system.

Bibliography

[1] National Energy Board, "Canada's Energy Future 2017", *Cat. No. NE2-12/2017E-PDF*, 2017

[2] "World Development Indicators — Data", *Online Source, Accessible from: data.worldbank.org. Retrieved 2016-09-17*

[3] International Renewable Energy Agency (IRENA), "Renewable capacity highlights 30 March 2017", *Online Source, Accessible from: resourceirena.irena.org*

[4] N. D. Kaushika, and N. K. Gautam, "Energy Yield Simulations of Interconnected Solar PV Arrays", *IEEE Trans. on Energy Conversion*, vol. 18, no. 1, Mar. 2003

[5] N. K. Gautam, and N.D. Kaushika, "An efficient algorithm to simulate the electrical performance of solar photovoltaic arrays", *Elsevier Energy*, vol. 27, no. 4, Apr. 2002, pp. 347-361

[6] H. Patel, and V. Agarwal, "MATLAB-Based Modeling to Study the Effects of Partial Shading on PV Array Characteristics", *IEEE Trans. on Energy Conversion*, vol. 23, no. 1, Mar. 2008

[7] R. Darussalam, R. I. Pramana, and A. Rajani, "Experimental Investigation of Serial Parallel and Total-Cross-Tied Configuration Photovoltaic Under Partial Shading Conditions", *2017 International Conference on Sustainable Energy Engineering and Application (ICSEEA)*, Oct. 2017

[8] H. S. Sahu, and S. K. Nayak, "Extraction of Maximum Power From a PV Array Under Nonuniform Irradiation Conditions", *IEEE Trans. on Electron Devices*, vol. 63, no. 12, Dec. 2016

[9] R. D. d. O. Reiter, L. Michels, J. R. Pinheiro, R. A. Reiter, S. V. G. Oliveira, and A. Peres, "Comparative Analysis of Series and Parallel Photovoltaic Arrays Under Partial Shading Conditions", *2012 10th IEEE/IAS International Conference on Industry Applications*, Nov. 2012

[10] W. Zhou, and K. Jin, "Optimal Photovoltaic Array Configuration Under Gaussian Laser Beam Condition for Wireless Power Transmission", *IEEE Trans. on Power Electronics*, vol. 32, no. 5, May 2017

[11] J. D. Bastidas-Rodriguez, C. A. Ramos-Paja, and L. A. Trejos-Grisales, "Mathematical Model of Bridge-Linked Photovoltaic Arrays Operating Under Irregular Conditions", *Revista Tecno Logicas*, pp. 223-235, 2013

[12] C. T. K. Kho, J. Ahmed, S. Kashem, and Y. L. Then, "A comprehensive review on PV configurations to maximize power under partial shading", *TENCON 2017 IEEE Region 10 Conference*, Nov. 2017

[13] M. Dhimish, V. Holmes, B. Mehrdadi, M. Dales, and P. Mather, "Output-Power Enhancement for Hot Spotted Polycrystalline Photovoltaic Solar Cells", *IEEE Trans. on Device and Materials Reliability*, vol. 18, no. 1, Mar. 2018

[14] C. A. Ramos-Paja, J. D. Bastidas, A. J. Saavedra-Montes, F. Guinjoan-Gispert, and M. Goez, "Mathematical model of total cross-tied photovoltaic arrays in mismatching conditions", *2012 IEEE 4th Colombian Workshop on Circuits and Systems (CWCAS)*, Nov. 2012

[15] H. Liu, L. Wan, and B. Pei, "Optimal Scheme of PV Array in Partial Shading : A Reconfiguration Algorithm", *2016 IEEE International Conference on Mechatronics and Automation*, China, Aug. 2016

[16] Y. Wang, X. Lin, Y. Kim, N. Chang, and M. Pedram, "Architecture and Control Algorithms for Combating Partial Shading in Photovoltaic Systems", *IEEE Trans. on Computer-aided Design of Integrated Circuits and Systems*, vol. 33, no. 6, Jun. 2014

[17] A. Kumar, R. K. Pachauri, and Y. K. Chauhan, "Experimental Analysis of SP/TCT PV Array Configurations under Partial Shading Conditions", *2016 IEEE 1st International Conference on Power Electronics, Intelligent Control and Energy Systems (ICPEICES)*, Jul. 2016

[18] F. Viola, P. Romano, R. Miceli, C. Spataro, and G. Schettino, "Technical and Economical Evaluation on the Use of Reconfiguration Systems in Some EU Countries for PV Plants", *IEEE Trans. on Industry Applications*, vol. 53, no. 2, Mar./Apr. 2017

[19] H. S. Sahu, S. K. Nayak, and S. Mishra, "Maximizing the Power Generation of a Partially Shaded PV Array", *IEEE Journal of Emerging and Selected topics in Power Electronics*, vol. 04, no. 2, Jun. 2016

[20] H. M. Hasanien, A. Al-Durra, and S. M. Muyeen, "Gravitational Search Algorithm-based Photovoltaic Array Reconfiguration for Partial Shading Losses Reduction", *5th IET International Conference on Renewable Power Generation (RPG) 2016*, Sept. 2016

[21] S. Moballegh, and J. Jiang, "Modeling, Prediction, and Experimental Validations of Power Peaks of PV Arrays Under Partial Shading Conditions", *IEEE Trans. on Sustainable Energy*, vol. 5, no. 1, Jan. 2014

[22] M. Amin, J. Bailey, C. Tapia, and V. Thodimeladine, "Comparison of PV Array Configuration Efficiency under Partial Shading Condition", *2017 IEEE 44th Photovoltaic Specialist Conference (PVSC)*, Jun. 2017

[23] C. Olalla, C. Deline, D. Clement, Y. Levron, M. Rodriguez, and D. Maksimovic, "Performance of Power-Limited Differential Power Processing Architectures in Mismatched PV Systems", *IEEE Trans. on Power Electronics*, vol. 30, no. 2, Feb. 2015

[24] M. A. A. Mamun, M. Hasanuzzaman, and J. Selvaraj, "Experimental investigation of the effect of partial shading on photovoltaic performance", *IET Renewable Power Generation*, vol. 11, no. 7, Jun. 2017

[25] X. Qing, H. Sun, X. Feng, and C. Y. Chung, "Submodule-Based Modeling and Simulation of a Series-Parallel Photovoltaic Array Under Mismatch Conditions", *IEEE Journal of Photovoltaics*, vol. 7, no. 6, Nov. 2017

[26] C. Rahmann, V. Vittal, J. Ascui, and J. Haas, "Mitigation Control Against Partial Shading Effects in Large-Scale PV Power Plants", *IEEE Trans. on Sustainable Energy*, vol. 7, no. 1, Jan. 2016

[27] A. Kumar; R. K. Pachauri, and Y. K. Chauhan, "Experimental analysis of proposed SP-TCT, TCT-BL and CT-HC configurations under partial shading conditions", *2016 IEEE 7th Power India International Conference (PIICON)*, Nov. 2016

[28] M. Z. S. El-Dein, M. Kazerani, and M. M. A. Salama, "Optimal Photovoltaic Array Reconfiguration to Reduce Partial Shading Losses", *IEEE Trans. on Sustainable Energy*, vol. 4, no. 1, Jan. 2013

[29] M. F. Jalil, R. Saxena, M. S. Ansari, and N. Ali, "Reconfiguration of Photo Voltaic Arrays under Partial Shading Conditions*", 2016 Second International Innovative Applications of Computational Intelligence on Power, Energy and Controls with their Impact on Humanity (CIPECH)*, Nov. 2016

[30] N. Rakesh, and U. Malavya, "Maximizing the Power Output of Partially Shaded Solar PV Array using Novel Interconnection Method", *International Conference on Innovative Mechanisms for Industry Applications (ICIMIA 2017)*, Feb. 2017

[31] I. Rani B, G. S. Ilango, and C. Nagamani, "Enhanced Power generation from PV array under partial shading conditions by shade dispersion using Su Do Ku configuration", *IEEE Trans. on Sustainable Energy vol. 4, no. 3*, Jul. 2013

[32] M. G. Villalva, J. R. Gazoli, and E. R. Filho, "Comprehensive Approach to Modeling and Simulation of Photovoltaic Arrays", *IEEE Trans. on Power Electronics*, vol. 24, no. 5, May 2009

[33] D. T. Lobera, and S. Valkealahti, "Mismatch Losses in PV Power Generators Caused by Partial Shading Due to Clouds", *2013 4th IEEE International Symposium on Power Electronics for Distributed Generation Systems (PEDG)*, Jul. 2013

[34] P. Sharma, and V. Agarwal, "Exact Maximum Power Point Tracking of Grid-Connected Partially Shaded PV Source Using Current Compensation Concept", *IEEE Trans. on Power Electronics*, vol. 29, no. 9, Sep. 2014

[35] A. D. Dhass; E. Natarajan; L. Ponnusamy, "Influence of Shunt Resistance on the Performance of Solar Photovoltaic Cell", *2012 International Conference on Emerging Trends in Electrical Engineering and Energy Management*, Dec. 2012

[36] L. Gao, R. A. Dougal, S. Liu, and A. P. Iotova, "Parallel-Connected Solar PV System to Address Partial and Rapidly Fluctuating Shadow Conditions*", IEEE Trans. on Industrial Electronics*, vol. 56, no. 5, May 2009

[37] E. Lorenzo, "Solar Electricity: Engineering of Photovoltaic Systems", *First English Edition, Progensa*, ISBN 84-86505-55-0, 1994

[38] N.D. Benavides, P.L. Chapman, "Modeling the effect of voltage ripple on the power output of photovoltaic modules", *IEEE Trans. on Industrial Electronics*, vol. 55, no. 7, Jul. 2008

[39] A. D. Rajapakse, D. Muthumuni, "Simulation tools for photovoltaic system grid integration studies", *2009 IEEE Electrical Power & Energy Conference (EPEC)*, Oct. 2009

[40] S. A. Arefifar, F. Paz, and M. Ordonez, "Improving Solar Power PV Plants Using Multivariate Design Optimization", *IEEE Journal of Emerging and Selected Topics in Power Electronics*, vol. 5, no. 2, Jun. 2017

[41] Krismadinataa, N. Abd. R. H. W. Pinga, and J. Selvaraj, "Photovoltaic module modeling using simulink/matlab", *The 3rd International Conference on Sustainable Future for Human Security SUSTAIN*, Nov. 2012

[42] N. Hayashi, A. Matsushita, D. Inoue, M. Matsumoto, T. Nagata, H. Higuchi, Y. Aya, and T. Nakagawa, "Nonuniformity Sunlight-Irradiation Effect on Photovoltaic Performance of Concentrating Photovoltaic Using Microsolar Cells Without Secondary Optics", *IEEE Journal of Photovoltaics,* vol. 6, no. 1, Jan. 2016

[43] I. Rani B, G. S. Ilango, and C. Nagamani, "Enhanced Power generation from PV array under partial shading conditions by shade dispersion using Su Do Ku configuration", *IEEE Trans. on Sustainable Energy*, vol. 4, no. 3, Jul. 2013

[44] S. Sumathi, "Solar PV and Wind Energy Conversion Systems, Green Energy and Technology", *Published in Springer International*, DOI 10.1007/978-3-319-14941-7˙2, Switzerland 2015

[45] D. Locke, "Guide to the Wiring Regulations 17th Edition IEE Wiring Regulations (BS 7671: 2008)", *Published in Wiley*, 2008

[46] V. P. Deshpande, and S. B. Bodkhe, "Analysis of Various Connection Configuration of Photovoltaic Module under Different Shading Condition", *International Journal of Applied Engineering Research*, vol. 12, no. 16, Jul. 2016, pp. 5715-5720

[47] C. McGee, "A study into the optimisation and calculation of electrical losses in renewable energy generation", *Thesis of Master of Science in Technology*, University of Strathclyde Engineering, 2014

[48] A. Maki, and S. Valkealahti, "Power Losses in Long String and Parallel-Connected Short Strings of Series-Connected Silicon-Based Photovoltaic Modules Due to Partial Shading Conditions", *IEEE Trans. on Energy Conversion*, vol. 27, no. 1, Mar. 2012

[49] T. Shimizu, M. Hirakata, T. Kamezawa, and H. Watanabe, "Generation control circuit for photovoltaic modules," *IEEE Trans. on Power Electronics*, vol. 16, no. 3, pp. 293–300, May 2001

[50] D. Nguyen and B. Lehman, "An adaptive solar photovoltaic array using model-based reconfiguration algorithm," *IEEE Trans. on Industrial Electronics*, vol. 55, no. 7, pp. 2644–2654, Jul. 2008

[51] C. Chang, "Solar cell array having lattice or matrix structure and method of arranging solar cells and panels," *U.S. Patent* 6 635 817, Oct. 21, 2003.

[52] R. A. Sherif and K. S. Boutros, "Solar module array with reconfigurable tile," *U.S. Patent* 6 350 944, Feb. 26, 2002.

[53] G. Velasco-Quesada, F. Guinjoan-Gispert, R. Pique-lopez, M. Roman-Lumbreras, and A. Conesa-Roca, "Electrical PV array reconfiguration strategy for energy extraction improvement in grid connected systems," *IEEE Trans. on Industrial Electronics*, vol. 56, no. 11, pp. 4319–4331, Nov. 2009

[54] Independent Electricity System Operator (IESO), "FIT/microFIT PRICE SCHEDULE", Jan. 2017, *Online at: http://www.ieso.ca/-/media/files/ieso/document-library/fit/2017-fit-price-schedule.pdf?la=en*

[55] M. Horoufiany, and R. Ghandehari, "Optimal fixed reconfiguration scheme for PV arrays power enhancement under mutual shading conditions", *IET Renewable Power Generation*, vol. 11, no. 11, Sep. 2017